# CANADIAN JOURNAL OF RESEARCH

VOLUME 17 JULY, 1939 NUMBER 7

## CONTENTS

### SEC. A.—PHYSICAL SCIENCES

Page

The Equilibrium of a Thin Compressible Membrane with Application to the Periodontal Membrane—*G. E. Hay* - 123

The Resonant Radial Frequencies of a Cylinder of Any Wall Thickness—*G. S. Field* - - - - - - - - - - 141

### SEC. B.—CHEMICAL SCIENCES

A Method for the Determination of Organic Phosphorus in Soils and Soil Extracts—*C. L. Wrenshall and W. J. Dyer* - - - 199

Pressure, Volume, Temperature Relations of Ethylene in the Critical Region. I.—*J. Dacey, R. McIntosh and O. Maass* - 206

NATIONAL RESEARCH COUNCIL
OTTAWA, CANADA

## Publications and Subscriptions

The Canadian Journal of Research is issued monthly in four sections, as follows;

A. Physical Sciences
B. Chemical Sciences
C. Botanical Sciences
D. Zoological Sciences

For the present, Sections A and B are issued under a single cover, as also are Sections C and D, with separate pagination of the four sections, to permit separate binding, if desired.

Subscription rates, postage paid to any part of the world (effective 1 April, 1939), are as follows:

| | *Annual* | *Single Copy* |
|---|---|---|
| A and B | $ 2.50 | $ 0.50 |
| C and D | 2.50 | 0.50 |
| Four sections, complete | 4.00 | — |

The Canadian Journal of Research is published by the National Research Council of Canada under authority of the Chairman of the Committee of the Privy Council on Scientific and Industrial Research. All correspondence should be addressed:

*National Research Council, Ottawa, Canada.*

## Notice to Contributors

Beginning with the September issue of the Canadian Journal of Research, fifty reprints of each paper will be supplied free.

Additional reprints, if required, will be supplied according to a schedule of charges to be announced.

# Canadian Journal of Research

*Issued by* THE NATIONAL RESEARCH COUNCIL OF CANADA

VOL. 17, SEC. A. JULY, 1939 NUMBER 7


## THE EQUILIBRIUM OF A THIN COMPRESSIBLE MEMBRANE WITH APPLICATION TO THE PERIODONTAL MEMBRANE[1]


BY G. E. HAY[2]



### Abstract

The equilibrium of a thin compressible elastic membrane has been considered. In the present work the theory developed in that paper (3) is applied to the periodontal membrane which lies between the tooth and the jaw-bone.

For simplicity, a tooth is considered of which the root is a right circular cone, the thickness of the membrane being assumed constant. A load is applied to the tooth in a plane containing the axis of the root and a determination is made of the resulting stress in the membrane and displacement of the tooth.

It is also found that the periodontal membrane holds the tooth in place in a way different from that commonly accepted by dentists.


### Introduction

In a preceding paper (3) the equilibrium of a thin compressible membrane has been considered. In the present paper the theory there developed is applied to the periodontal membrane which lies between the tooth and the jaw-bone and is attached to both. The theory is applicable to multiple-rooted as well as single-rooted teeth but only the latter type will be considered, in particular the upper central incisor which has the following average measurements (1, p. 19):—

| | |
|---|---|
| Length over all | 0.88 in. |
| Crown length | 0.39 in. |
| Root length | 0.49 in. |
| Mesio-distal diameter at neck (side to side) | 0.24 in. |
| Labio-lingual diameter at neck (front to back) | 0.27 in. |

The ayerage thickness of the periodontal membrane is from 0.0091 to 0.0099 in. (6, p. 123).

The equilibrium of the periodontal membrane considered as incompressible has been considered by J. L. Synge (8), and there is an interesting comparison between his results and those of this paper.

In the author's preceding paper (3, §3) there was introduced the equation

$$1-2\sigma=k\epsilon^n, \tag{1.1}$$


[1] *Original manuscript received September 28, 1938.*

*Contribution from the Department of Applied Mathematics, University of Toronto, Toronto, Canada.*


[2] *Holder of a Bursary under the National Research Council of Canada.*

where $\sigma$ was Poisson's ratio, $\epsilon$ was a small dimensionless parameter defined by

$$\epsilon=\frac{\text{average thickness of the membrane}}{\text{average length of the membrane}}, \tag{1.2}$$

and $n$ was an integer to be so chosen that $k$ was comparable with unity. Owing to the method of approximation used in solving the equations of equilibrium, different results were obtained in the four cases $n=0$, 1, 2, and $n>2$. The first step is thus to determine which case applies to the periodontal membrane, for which the following average values may be taken

$$\begin{cases}\epsilon=2\times10^{-2}, \quad \epsilon^2=4\times10^{-4}, \quad \epsilon^3=8\times10^{-6},\\ \mu=\text{rigidity (2)}=73 \text{ lb. in.}^{-2}\end{cases} \tag{1.3}$$

Since the human body is composed largely of water it seems logical to take for the bulk modulus of the membrane that of water

$$\kappa=2.96\times10^5 \text{ lb. in.}^{-2} \tag{1.4}$$

Hence

$$1-2\sigma=\frac{3\mu}{3\kappa+\mu}=2.5\times10^{-4}, \tag{1.5}$$

and so if $n=1,2,3$, the respective values of $k$ are

$$\begin{cases}k=(1-2\sigma)/\epsilon=1.2\times10^{-2},\\ k=(1-2\sigma)/\epsilon^2=0.6,\\ k=(1-2\sigma)/\epsilon^3=30.\end{cases} \tag{1.6}$$

Thus it appears that the case $n=2$ applies to the periodontal membrane. This case has been investigated (3, §8): it was found that the principal part of the stress in the membrane was a hydrostatic pressure satisfying a partial differential equation (3, Equation (8.22) ), subject to the boundary condition that the pressure at the free edge be atmospheric. This differential equation appears in a modified form in §2 and is solved in §3 for a restricted shape of tooth.

## 2. The Tooth of Revolution. The Pressure in the Membrane Expressed by the Solution of Three Ordinary Differential Equations

For a general tooth the partial differential equation satisfied by the pressure is rather complicated. The case will now be considered when the socket $S$ and tooth $T$ both have surfaces of revolution about a common axis. This implies that the thickness of the membrane has the same symmetry of revolution. The edge of the membrane is assumed to be a circle normal to the axis of revolution, although in practice this is not realized very closely.

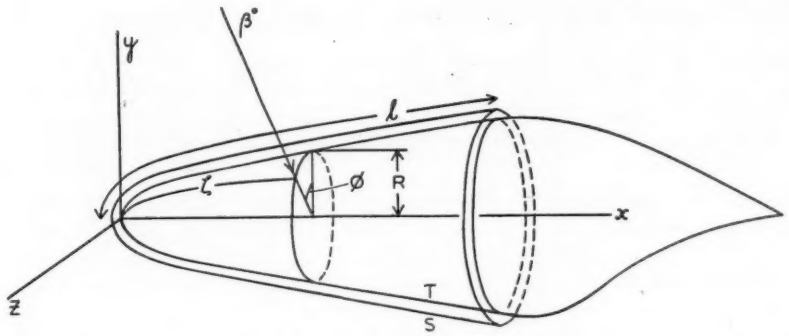


FIG. 1. *Model of a tooth and periodontal membrane.*

A set of rectangular cartesian axes are taken with the origin at the apex, the axis of $x$ being coincident with the axis of revolution. A set of surface co-ordinates $\zeta$ and $\phi$ are also taken over $S$ where $\zeta$ is the meridian distance from the apex and $\phi$ is the azimuth measured from the plane $z=0$. Then the partial differential equation for the pressure $p$ in the membrane [3, Equation (8.22)] takes the form

$$\frac{1}{R}\frac{\partial}{\partial\zeta}\left(Rh^3\frac{\partial p}{\partial\zeta}\right)+\frac{h^3}{R^2}\frac{\partial^2 p}{\partial\phi^2}-12(1-2\sigma)hp=4E\beta^0; \tag{2.1}$$

the boundary conditions are the following,

$$\begin{cases} \text{for } \zeta=0,\ p \text{ must be single valued,} \\ \text{for } \zeta=l,\ p=P; \end{cases} \tag{2.2}$$

and $R$ is the radius of a general section normal to the axis of $x$, $h$ is the thickness of the membrane, $E$ is Young's modulus, $\sigma$ is Poisson's ratio, $\beta^0$ is the component normal to $S$ of the displacement of a point on $T$, counted positive when in the sense from $S$ to $T$, $l$ is the meridian length of the membrane and $P$ is atmospheric pressure.

In (2.1) $\beta^0$ is a function of $\zeta$ and $\phi$ and is known when the infinitesimal rigid body displacement of $T$ is known. To find it, the displacement of $T$ is resolved into infinitesimal translations $u$, $v$ and $w$ in the directions of the axes and infinitesimal rotations $\omega_1$, $\omega_2$, and $\omega_3$ about them. Then the displacement of a point $(x, y, z)$ on $T$ has components

$$u-y\omega_3+z\omega_2, \qquad v-z\omega_1+x\omega_3, \qquad w-x\omega_2+y\omega_1,$$

and hence

$$\begin{aligned}\beta^0=u\frac{dR}{d\zeta}&-\cos\phi\left\{v\frac{dx}{d\zeta}+\omega_3\left(x\frac{dx}{d\zeta}+R\frac{dR}{d\zeta}\right)\right\}\\&-\sin\phi\left\{w\frac{dx}{d\zeta}-\omega_2\left(x\frac{dx}{d\zeta}+R\frac{dR}{d\zeta}\right)\right\}.\end{aligned} \tag{2.3}$$

Thus (2.1) can be written in the form

$$(2.4)\qquad \frac{1}{R}\frac{\partial}{\partial\zeta}\left(Rh^3\frac{\partial p}{\partial\zeta}\right)+\frac{h^3}{R^2}\frac{\partial^2 p}{\partial\phi^2}-12(1-2\sigma)hp$$
$$=4Eu\frac{dR}{d\zeta}-4E\cos\phi\left\{v\frac{dx}{d\zeta}-\omega_3\left(x\frac{dx}{d\zeta}+R\frac{dR}{d\zeta}\right)\right\}$$
$$-4E\sin\phi\left\{w\frac{dx}{d\zeta}-\omega_2\left(x\frac{dx}{d\zeta}+R\frac{dR}{d\zeta}\right)\right.$$

It is to be noted that $\omega_1$ does not appear in (2.4), since it contributes nothing to $\beta^0$.

Except for $\cos\phi$ and $\sin\phi$ the right-hand side of (2.4) is a known function of $\zeta$ and the solution of (2.4) must then have the form

$$(2.5)\qquad p=f(\zeta)+\cos\phi g(\zeta)+\sin\phi g'(\zeta).$$

Upon substitution of this in (2.4) a differential equation is obtained for each of $f$, $g$ and $g'$, whence follows the result:—

I. In the case of a tooth of revolution the pressure in the periodontal membrane is given by (2.5) where $f$, $g$ and $g'$ satisfy the equations

$$(2.6)\qquad \frac{1}{R}\frac{d}{d\zeta}\left(Rh^3\frac{df}{d\zeta}\right)-12(1-2\sigma)hf=4Eu\frac{dR}{d\zeta},$$

$$(2.7)\qquad \frac{1}{R}\frac{d}{d\zeta}\left(Rh^3\frac{dg}{d\zeta}\right)-\left\{\frac{h^3}{R^2}+12(1-2\sigma)h\right\}g$$
$$=-4E\left\{v\frac{dx}{d\zeta}+\omega_3\left(x\frac{dx}{d\zeta}+R\frac{dR}{d\zeta}\right)\right\},$$

$$(2.8)\qquad \frac{1}{R}\frac{d}{d\zeta}\left(Rh^3\frac{dg'}{d\zeta}\right)-\left\{\frac{h^3}{R^2}+12(1-2\sigma)h\right\}g'$$
$$=-4E\left\{w\frac{dx}{d\zeta}-\omega_2\left(x\frac{dx}{d\zeta}+R\frac{dR}{d\zeta}\right)\right\},$$

with the boundary conditions

$$(2.9)\qquad f(0)\text{ must be finite, }f(l)=P,$$
$$(2.10)\qquad g(0)=g(l)=0,$$
$$(2.11)\qquad g'(0)=g'(l)=0.$$

In these formulae $R$, $\zeta$, $\phi$, $x$ and $l$ are as shown in Fig. 1, $h$ is the thickness of the membrane, $E$ is Young's modulus, $\sigma$ is Poisson's ratio and the infinitesimal rigid body displacement is specified by the translation $(u, v, w)$ and the rotation $(\omega_1, \omega_2, \omega_3)$ relative to the axes of $x$, $y$ and $z$ in Fig. 1.

## 3. The Conical Model under Plane Displacement

A tooth of which the root is a right circular cone will now be considered. This is the simplest geometrical figure which can be chosen to represent the average shape of a single-rooted tooth. The rest of the paper is confined to membranes of uniform thickness $h$, although the thickness varies considerably in the human tooth.

Only plane displacements of the tooth will be considered, *i.e.*, displacements in which the axis of the tooth remains in a plane, and the axis of $y$ will be chosen to lie in this plane. Hence in the notation of §2,

$$w=\omega_1=\omega_2=0. \tag{3.1}$$

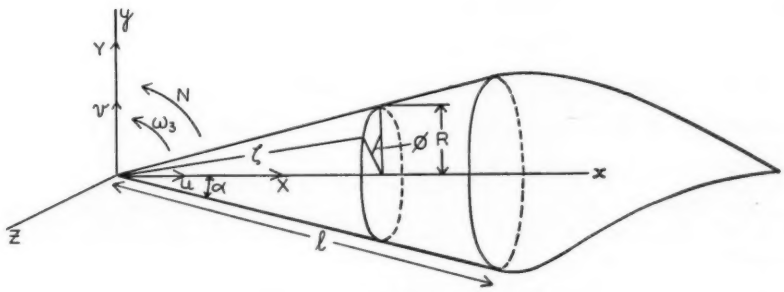


FIG. 2. *Conical model of a tooth.*

Fig. 2 shows the conical model for which

$$R=\zeta \sin\alpha, \qquad x=\zeta\cos\alpha, \tag{3.2}$$

and substitution from (3.1) and (3.2) in (2.6), (2.7) and (2.8) gives

$$h^3\frac{d^2f}{d\zeta^2}+\frac{h^3}{\zeta}\frac{df}{d\zeta}-12(1-2\sigma)hf=4Eu\sin\alpha, \tag{3.3}$$

$$h^3\frac{d^2g}{d\zeta^2}+\frac{h^3}{\zeta}\frac{dg}{d\zeta}-\left\{12(1-2\sigma)h+\frac{h^3}{\zeta^2\sin^2\alpha}\right\}g =-4E(v\cos\alpha+\omega_3\zeta), \tag{3.4}$$

$$h^3\frac{d^2g'}{d\zeta^2}+\frac{h^3}{\zeta}\frac{dg'}{d\zeta}-\left\{12(1-2\sigma)h+\frac{h^3}{\zeta^2\sin^2\alpha}\right\}g'=0. \tag{3.5}$$

A variable $\zeta_1$, a constant $l_1$ and the functions $f_1$, $g_1$ and $g_1'$ are defined as follows:—

$$\zeta_1=\nu\zeta, \qquad l_1=\nu l, \tag{3.6}$$

$$f_1(\zeta_1)=f(\zeta), \qquad g_1(\zeta_1)=g(\zeta), \qquad g_1'(\zeta_1)=g'(\zeta), \tag{3.7}$$

where

$$\nu=\sqrt{12(1-2\sigma)}/h. \tag{3.8}$$

Then the differential equations (3.3), (3.4) and (3.5) take the forms

$$\zeta_1^2 \frac{d^2 f_1}{d\zeta_1^2} + \zeta_1 \frac{df_1}{d\zeta_1} - \zeta_1^2(G+f_1) = 0, \tag{3.9}$$

$$\zeta_1^2 \frac{d^2 g_1}{d\zeta_1^2} + \zeta_1 \frac{dg_1}{d\zeta_1} - (\operatorname{cosec}^2\alpha + \zeta_1^2) g_1 = C\zeta_1^2 - D\zeta_1^3, \tag{3.10}$$

$$\zeta_1^2 \frac{d^2 g_1'}{d\zeta_1^2} + \zeta_1 \frac{dg_1'}{d\zeta_1} - (\operatorname{cosec}^2\alpha + \zeta_1^2) g_1' = 0. \tag{3.11}$$

The boundary conditions obtained from (2.9), (2.10) and (2.11) are

$$f_1(0) \text{ must be finite, } f_1(l_1) = P, \tag{3.12}$$

$$g_1(0) = g_1(l_1) = 0, \tag{3.13}$$

$$g_1'(0) = g_1'(l_1) = 0, \tag{3.14}$$

where $G$, $C$, and $D$ are the constants

$$G = 4Eu \sin\alpha/(h^3\nu^2), \quad C = -4Ev\cos\alpha/(h^3\nu^2), \quad D = -4E\omega_3/(h^3\nu^3), \tag{3.15}$$

and all other quantities are defined in I.

Solutions for (3.9), (3.10) and (3.11) will be obtained in turn. Since (3.9) is Bessel's modified equation of order zero, the solution satisfying the boundary condition (3.12) is

$$f_1(\zeta_1) = -G + (P+G) I_0(\zeta_1)/I_0(l_1), \tag{3.16}$$

where

$$I_0(\zeta_1) = \sum_{m=0}^{\infty} \frac{(\frac{1}{2}\zeta_1)^{2m}}{(m!)^2}, \qquad (0! = 1). \tag{3.17}$$

In the course of solving (3.10) it is found that the form of the solution is different in the three cases (i) cosec $\alpha \neq$ integer, (ii) cosec $\alpha$ = odd integer, (iii) cosec $\alpha$ = even integer. Since $\alpha$ is the semi-angle of the root cone, the arithmetical values in §1 give cosec $\alpha = 4.0$. Thus a solution will be required in Case (iii) only, in which case

$$\operatorname{cosec}\alpha = 2n, \qquad (n = 1, 2, \ldots). \tag{3.18}$$

The left-hand side of (3.10) is then Bessel's modified equation of order $2n$ and the complete solution of (3.10) is

$$g_1(\zeta_1) = D\psi(\zeta_1) + C\chi(\zeta_1) + AI_{2n}(\zeta_1) + BK_{2n}(\zeta_1), \tag{3.19}$$

where $A$ and $B$ are arbitrary constants, $D$ and $C$ are the known constants defined in (3.15), $I_{2n}(\zeta_1)$ and $K_{2n}(\zeta_1)$ are Bessel functions and $\psi$ and $\chi$ are any solutions of

$$\zeta_1^2 \frac{d^2\psi}{d\zeta_1^2} + \zeta_1 \frac{d\psi}{d\zeta_1} - (4n^2 + \zeta_1^2)\psi = \zeta_1^3, \tag{3.20}$$

$$\zeta_1^2 \frac{d^2\chi}{d\zeta_1^2} + \zeta_1 \frac{d\chi}{d\zeta_1} - (4n^2 + \zeta_1^2)\chi = \zeta_1^2. \tag{3.21}$$

When $n$ is an integer (3.20) has the solution in series*

$$\psi(\zeta_1)=\sum_{m=1}^{\infty}\frac{\zeta_1^{2m+1}}{\prod_{r=1}^{m}\{(2r+1)^2-4n^2\}}, \tag{3.22}$$

and (3.21) has the solution in series**

$$\begin{aligned}\chi(\zeta_1)=&\sum_{m=1}^{n-1}\frac{\zeta_1^{2m}}{\prod_{r=1}^{m}\{(2r)^2-4n^2\}}\\&+\frac{\log_e\zeta_1}{4n\prod_{r=1}^{n-1}\{(2r)^2-4n^2\}}\left[\zeta_1^{2n}+\sum_{m=n+1}^{\infty}\frac{\zeta_1^{2m}}{\prod_{r=n+1}^{m}\{(2r)^2-4n^2\}}\right]\\&-\sum_{m=n}^{\infty}\left[\frac{1}{4n}+\sum_{r=1}^{m}{}'\frac{4r}{(2r)^2-4n^2}\right]\frac{\zeta_1^{2m}}{4n\prod_{r=1}^{m}{}'\{(2r)^2-4n^2\}},\end{aligned} \tag{3.23}$$

where the dash on the $\Pi$ and $\Sigma$ signs means that the terms $r=n$ are to be omitted. Using the boundary conditions (3.13), a determination can be made of $A$ and $B$, whence

$$g_1(\zeta_1)=D\psi(\zeta_1)+C\chi(\zeta_1)-\{D\psi(l_1)+C\chi(l_1)\}I_{2n}(\zeta_1)/I_{2n}(l_1). \tag{3.24}$$

It is noted that

$$I_{2n}(\zeta_1)=\sum_{m=0}^{\infty}\frac{(\frac{1}{2}\zeta_1)^{2(m+n)}}{m!(m+2n)!}, \qquad (n=1, 2, \ldots). \tag{3.25}$$

Since (3.11) is Bessel's modified equation of order $2n$, it has the complete solution

$$g_1'(\zeta_1)=A'I_{2n}(\zeta_1)+B'K_{2n}(\zeta_1), \tag{3.26}$$

where $A'$ and $B'$ are arbitrary constants. Using the boundary conditions (3.14), it is found that $A'=B'=0$, whence

$$g_1'(\zeta_1)\equiv 0. \tag{3.27}$$

These results are summed up as follows:—

II. For a conical model of a tooth subjected to the plane displacement specified by $u$, $v$, and $\omega_3$ as shown in Fig. 2, the pressure in the periodontal membrane is given by

$$p(\zeta_1)=f_1(\zeta_1)+\cos\phi g_1(\zeta_1), \tag{3.28}$$

* *This is derived in Appendix A.*

** *This is derived in Appendix B.*

where

$$f_1(\zeta_1) = -G + (P+G) I_0(\zeta_1)/I_0(l_1)\,,$$

$$g_1(\zeta_1) = D\psi(\zeta_1) + C\chi(\zeta_1) - \{D\psi(l_1) + C\chi(l_1)\} I_{2n}(\zeta_1)/I_{2n}(l_1)\,,$$

$$G = 4Eu \sin\alpha/(h^3\nu^2), \quad C = -4Ev\cos\alpha/(h^3\nu^2), \quad D = -4E\omega_3/(h^3\nu^3)\,,$$

$$\nu = \sqrt{12(1-2\sigma)}/h, \qquad \operatorname{cosec}\alpha = 2n, \qquad (n = \text{integer}),$$

and $\psi(\zeta_1)$, $\chi(\zeta_1)$ and $I_{2n}(\zeta_1)$ are defined in (3.22), (3.23) and (3.25) respectively.

In these formulae $\phi$ is the azimuth measured from the plane $z=0$ of the displacement (Fig. 2), $P$ is atmospheric pressure, $E$ is Young's modulus, $\sigma$ is Poisson's ratio, $h$ is the thickness of the membrane and is a constant, $\alpha$ is the semi-angle of the root cone and $\zeta_1$ is a co-ordinate running along a generator of the root cone, having the value zero at the apex and at the edge of the membrane the value $l_1 = \nu l$, where $l$ is the slant length of the root cone.

The external force system, exclusive of atmospheric pressure, acting on the tooth and producing such a pressure $p$ in the membrane is statically equivalent to forces $X$ and $Y$ acting along the axes of $x$ and $y$ respectively and a couple $N$ acting about the axis of $z$: thus

$$(3.29)\quad \begin{cases} X = -\displaystyle\int_{\zeta=0}^{l}\int_{\phi=0}^{2\pi} (p-P)\zeta \sin^2\alpha \, d\zeta \, d\phi\,, \\ Y = \displaystyle\int_{\zeta=0}^{l}\int_{\phi=0}^{2\pi} (p-P)\zeta \sin\alpha\cos\alpha\cos\phi \, d\zeta \, d\phi\,, \\ N = \displaystyle\int_{\zeta=0}^{l}\int_{\phi=0}^{2\pi} (p-P)\zeta^2 \sin\alpha\cos\phi \, d\zeta \, d\phi\,. \end{cases}$$

Since $\zeta_1 = \nu\zeta$ substitution for $p$ from II and easy integration gives the following result:—

III. The external force system necessary to produce the pressure distribution in II is statically equivalent to the force system ($X$, $Y$, $N$), (Fig. 2), and

$$(3.30)\quad X = \frac{\pi}{\nu^2}(P+G)\sin^2\alpha\{l_1^2 - 2I_{0,1}(l_1)/I_0(l_1)\},$$

$$(3.31)\quad Y = \frac{\pi}{\nu^2}\sin\alpha\cos\alpha\{D\psi_1(l_1) + C\chi_1(l_1) - [D\psi(l_1) + C\chi(l_1)]I_{2n,1}(l_1)/I_{2n}(l_1)\},$$

$$(3.32)\quad N = \frac{\pi}{\nu^3}\sin\alpha\{D\psi_2(l_1) + C\chi_2(l_1) - [D\psi(l_1) + C\chi(l_1)]I_{2n,2}(l_1)/I_{2n}(l_1)\},$$

where

$$(3.33)\qquad I_{2n,t}(l_1)=\int_0^{l_1}\zeta_1{}^t I_{2n}(\zeta_1)\,d\zeta_1\,,$$

$$=2^{t+1}\sum_{m=0}^{\infty}\frac{(\frac{1}{2}l_1)^{2m+2n+t+1}}{(2m+2n+t+1)m!(m+2n)!}\,,$$

$$(0!=1,\quad n=0,\,1,\,\ldots\,,\quad t=1,\,2),$$

$$(3.34)\qquad \psi_t(l_1)=\int_0^{l_1}\zeta_1{}^t\psi(\zeta_1)\,d\zeta_1\,,$$

$$=\sum_{m=1}^{\infty}\frac{l_1{}^{2m+t+2}}{(2m+t+2)\prod_{r=1}^{m}\{(2r+1)^2-4n^2\}}\,,\qquad (t=1,\,2),$$

$$(3.35)\qquad \chi_t(l_1)=\int_0^{l_1}\zeta_1{}^t\chi(\zeta_1)\,d\zeta_1\,,$$

$$=\sum_{m=1}^{n-1}\frac{l_1{}^{2m+t+1}}{(2m+t+1)\prod_{r=1}^{m}\{(2r)^2-4n^2\}}$$

$$+\frac{\log_e l_1}{4n\prod_{r=1}^{n-1}\{(2r)^2-4n^2\}}\left[\frac{l_1{}^{2n+t+1}}{2n+t+1}+\sum_{m=n+1}^{\infty}\frac{l_1{}^{2m+t+1}}{(2m+t+1)\prod_{r=n+1}^{m}\{(2r)^2-4n^2\}}\right]$$

$$-\frac{1}{4n\prod_{r=1}^{n-1}\{(2r)^2-4n^2\}}\left[\frac{l_1{}^{2n+t+1}}{(2n+t+1)^2}+\sum_{m=n+1}^{\infty}\frac{l_1{}^{2m+t+1}}{(2m+t+1)^2\prod_{r=n+1}^{m}\{(2r)^2-4n^2\}}\right]$$

$$-\sum_{m=n}^{\infty}\left[\frac{1}{4n}+\sum_{r=1}^{m}{}'\frac{4r}{(2r)^2-4n^2}\right]\frac{l_1{}^{2m+t+1}}{4n(2m+t+1)\prod_{r=1}^{m}{}'\{(2r)^2-4n^2\}}\,,\quad (t=1,\,2)\,,$$

and the notation is as in II, the dash on the $\Sigma$ and $\Pi$ signs again indicating that the terms $r=n$ are to be omitted.

The following values consistent with one another and with the physical data are assumed as the basis for calculation:

$$(3.36)\qquad \begin{cases} b=\text{over-all length of tooth} & =0.88\text{ in.}\\ l=\text{slant length of root cone} & =0.50\text{ in.}\\ \alpha=\text{semi-angle of root cone} & =\sin^{-1}\frac{1}{4}.\\ h=\text{thickness of membrane} & =0.0098\text{ in.}\\ \nu=\sqrt{12(1-2\sigma)}/h & =5.6\text{ in.}^{-1} \end{cases}$$

In §5, on account of the cancellation of positive and negative terms, it is found necessary to work initially with eight-figure accuracy in order to obtain three significant figures in the result.

## 4. The Conical Model Subjected to a Force $X$ Acting on the Crown and Parallel to the Axis of the Root

The crown is assumed to lie on the axis of the root. The tooth then undergoes an axial displacement only, and in the notation of §3,

$$Y=N=0, \qquad v=\omega_3=0, \qquad C=D=0. \tag{4.1}$$

Since $G=4Eu \sin\alpha/(h^3\nu^2)$ the axial displacement is, from (3.30),

$$u=\frac{h^3\nu^2}{4E\sin\alpha}\left[-P+\frac{X\nu^2}{\pi\sin^2\alpha}\{l_1^2-2I_{0,1}(l_1)/I_0(l_1)\}^{-1}\right], \tag{4.2}$$

and in terms of $u$ the pressure distribution is, from II,

$$p(\zeta_1)=-\frac{4Eu\sin\alpha}{h^3\nu^2}+\left(P+\frac{4Eu\sin\alpha}{h^3\nu^2}\right)\frac{I_0(\zeta_1)}{I_0(l_1)}. \tag{4.3}$$

It is to be noted that the membrane is in the unstressed state when the external load and the atmospheric pressure both vanish. When $X=0$ the whole system (tooth, membrane and jaw) is subject to atmospheric pressure $P$ only, and the axial displacement, which will be denoted by $\bar{u}$, is

$$\bar{u}=-Ph^3\nu^2/(4E\sin\alpha). \tag{4.4}$$

Then from (4.3) and (4.4),

$$p(\zeta_1)=-4E\bar{u}\sin\alpha/(h^3\nu^2)=P, \tag{4.5}$$

*i.e.*, the pressure throughout the membrane is atmospheric.

The points of maximum pressure in the membrane will now be determined for a general axial load on the tooth. The pressure at the edge of the membrane is always atmospheric, and, since the gradient of $I_0(\zeta_1)$ is positive, from (4.3) it can be seen that

$$\frac{dp}{d\zeta_1}>0 \text{ or } <0 \text{ according as } P+4Eu\sin\alpha/(h^3\nu^2)>0 \text{ or } <0.$$

Substitution for $u$ from (4.2) gives

$$\frac{dp}{d\zeta_1}>0 \text{ or } <0 \text{ according as } X\{l_1^2-2I_{0,1}(l_1)/I_0(l_1)\}^{-1}>0 \text{ or } <0.$$

Using the values in (3.36), it is found that $l_1=2.80$, $I_0(l_1)=4.16$ and $I_{0,1}(l_1)=9.24$, whence $l_1^2-2I_{0,1}(l_1)/I_0(l_1)=3.40$. Thus

$$\frac{dp}{d\zeta_1}>0 \text{ or } <0 \text{ according as } X>0 \text{ or } <0.$$

These results are summed up as follows:—

IV. When the external load acts from apex to crown the minimum pressure occurs at the apex and the maximum at the edge of the membrane. When the external load acts from crown to apex the minimum pressure occurs at the edge of the membrane and the maximum at the apex. In each case the

pressure at the edge of the membrane is atmospheric and the pressure at the apex is

$$(4.6) \qquad p(0)=P-\frac{X\nu^2}{\pi\sin^2\alpha}\{1-1/I_0(l_1)\}\{l_1^2-2I_{0,1}(l_1)/I_0(l_1)\}^{-1},$$

where $P$ is atmospheric pressure, $\nu=5.6$ in.$^{-1}$, $l_1=2.8$, $I_0(l_1)=4.16$, $I_{0,1}(l_1)=9.24$ and $\sin\alpha=\frac{1}{4}$.

A diagram will now be constructed illustrating the pressure variation along a generator of the root cone when $X$ is such that, (*i*) $p(0)=2P$, (*ii*) $p(0)=0$.

When $p(0)=2P$, the external load will be denoted by $X'$, the corresponding displacement by $u'$ and the corresponding pressure by $p'(\zeta_1)$. From (4.6) it is found that

$$(4.7) \qquad X'=-\frac{\pi}{\nu^2}P\sin^2\alpha\{l_1^2-2I_{0,1}(l_1)/I_0(l_1)\}\{1-1/I_0(l_1)\}^{-1},$$

and hence by (4.2),

$$(4.8) \qquad u'=-\frac{Ph^3\nu^2}{4E\sin\alpha}\frac{2I_0(l_1)-1}{I_0(l_1)-1}.$$

Finally from (4.3),

$$(4.9) \qquad p'(\zeta_1)=P\{2I_0(l_1)-1-I_0(\zeta_1)\}\{I_0(l_1)-1\}^{-1}.$$

When $p(0)=0$, the external load will be denoted by $X''$, the corresponding displacement by $u''$ and the corresponding pressure by $p''(\zeta_1)$. It is found that

$$(4.10) \qquad X''=-X', \qquad u''=-u', \qquad p''(\zeta_1)=2P-p'(\zeta_1).$$

To compute $u'$ and $u''$ requires Young's modulus for the membrane. Since $\sigma=\frac{1}{2}$, approximately, then $E=3\mu$:
since $\mu$ is known (2)

$$(4.11) \qquad E=219 \text{ lb. in.}^{-2}$$

When $P=$ 15 lb. in.$^{-2}$ the values in (3.36) give

$$(4.12) \qquad \begin{cases} X'=-X''=-0.42 \text{ lb.}, \\ u'=-u''=-2.65\times10^{-6} \text{ in.}, \\ \bar{u}=-1.99\times10^{-6} \text{ in.} \end{cases}$$

The graphs of $p'(\zeta_1)$ and $p''(\zeta_1)$ are shown in Fig. 3.

When the membrane is incompressible the corresponding values derived by Synge (8) are

$$(4.13)\quad \begin{cases} X' = -X'' = -0.38 \text{ lb.}, \\ u' = -u'' = -8.8\times10^{-7} \text{ in.}, \end{cases}$$

and the graphs corresponding to $p'(\zeta_1)$ and $p''(\zeta_1)$ are shown in Fig. 3.

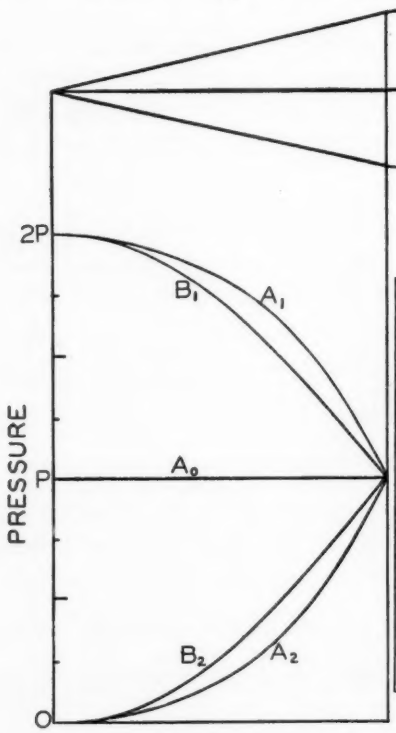


| | Compressible membrane | Incompressible membrane |
|---|---|---|
| X | -0.42 lb. | -0.38 lb. |
| u | $-4.64\times10^{-6}$ in. | $-8.8\times10^{-7}$ in. |
| Pressure dist'n. | $A_1$ | $B_1$ |
| X | 0.00 lb. | |
| u | $-1.99\times10^{-6}$ in. | |
| Pressure dist'n. | $A_0$ | |
| X | 0.42 lb. | 0.38 lb. |
| u | $6.6\times10^{-7}$ in. | $8.8\times10^{-7}$ in. |
| Pressure dist'n. | $A_2$ | $B_2$ |

$P$ = atmospheric pressure (= 15 lb. in.$^{-2}$),
$X$ = external load,
$u$ = displacement due to $X$ and atmospheric pressure.

In the case of the compressible membrane the total displacement $u$ is made up of a part due to atmospheric pressure and a part due to the load $X$. When $X = -0.42$ lb., the part due to atmospheric pressure is $-1.99\times10^{-6}$ in. and the part due to $X$ is $-2.65\times10^{-6}$ in.

FIG. 3. *Conical model under axial load.*

## 5. The Conical Model Subjected to a Force $Y$ Acting on the Crown and Perpendicular to the Axis of the Root

The calculations in this section must be carried out initially to eight figures, as explained at the end of §3. The crown is again assumed to lie on the axis

of the tooth. Then, in the notation of §3, $X=0$ and $N=bY$, where $b$ is the over-all length of the tooth. Hence from (3.30), (3.31) and (3.32),

$$P+G=0, \tag{5.1}$$

$$C\alpha_1+D\beta_1=Y\nu^2/(\pi \sin\alpha \cos\alpha), \tag{5.2}$$

$$C\alpha_2+D\beta_2=bY\nu^2/(\pi \sin\alpha), \tag{5.3}$$

where

$$\left\{\begin{array}{ll} \alpha_1=\chi_1(l_1)-\chi(l_1)I_{2n,1}(l_1)/I_{2n}(l_1), & \beta_1=\psi_1(l_1)-\psi(l_1)I_{2n,1}(l_1)/I_{2n}(l_1), \\ \alpha_2=\chi_2(l_1)-\chi(l_1)I_{2n,2}(l_1)/I_{2n}(l_1), & \beta_2=\psi_2(l_1)-\psi(l_1)I_{2n,2}(l_1)/I_{2n}(l_1), \end{array}\right. \tag{5.4}$$

and the remaining notation is defined in II and (3.33), (3.34) and (3.35).

Numerical values are now introduced from (3.36). Then $n=2$ and the following values can be computed:—

$$\left\{\begin{array}{ll} I_4(l_1)=0.234\ 079\ 08, & \psi(l_1)=-\ 6.601\ 251\ 5, \\ & \chi(l_1)=-1.618\ 780\ 30, \\ I_{4,1}(l_1)=0.279\ 338\ 86, & \psi_1(l_1)=-\ 8.601\ 708\ 7, \\ & \chi_1(l_1)=-2.309\ 403\ 8, \\ I_{4,2}(l_1)=0.677\ 170\ 52, & \psi_2(l_1)=-20.547\ 149, \\ & \chi_2(l_1)=-5.407\ 079\ 8, \end{array}\right. \tag{5.5}$$

whence

$$\left\{\begin{array}{ll} \alpha_1=-0.377\ 628\ 3, & \beta_1=-0.724\ 088\ 6, \\ \alpha_2=-0.724\ 088\ 5, & \beta_2=-1.450\ 300. \end{array}\right. \tag{5.6}$$

The solution of (5.2) and (5.3) is thus

$$C/Y=3\ 537.441, \qquad D/Y=-1\ 901.81, \tag{5.7}$$

and using (5.1), the pressure distribution is, from II,

$$p(\zeta_1)-P=Y\cos\phi[-1901.81\psi(\zeta_1)+3537.44\chi(\zeta_1)-29170I_4(\zeta_1)], \tag{5.8}$$

where $\zeta_1$ runs from zero at the apex to 2.8 at the free edge, $\phi$ is the azimuth as shown in Fig. 2 and $\psi(\zeta_1)$, $\chi(\zeta_1)$ and $I_4(\zeta_1)$ are defined in (3.22), (3.23) and (3.25) respectively. The graph of $p(\zeta_1)$ is shown in Fig. 4. The maximum pressure occurs at $M$ and $N$, and it is found that the external load necessary to produce a maximum pressure of two atmospheres (30 lb. in.$^{-2}$) is

$$Y=0.188 \text{ lb.} \tag{5.9}$$

From Synge (8) the corresponding load for the incompressible membrane is $Y=0.190$ lb.

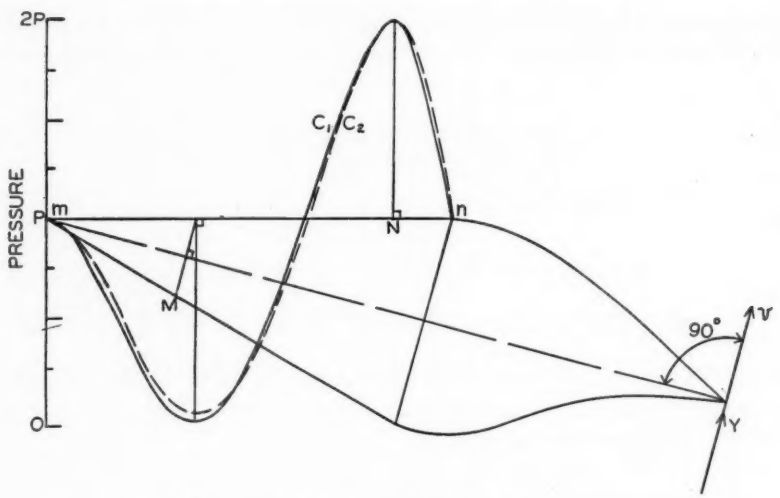


$P$ = atmospheric pressure (= 15 lb. in.$^{-2}$),
$Y$ = external load,
$v$ = displacement produced by $Y$.

| | Compressible membrane | Incompressible membrane |
|---|---|---|
| Apex to centre of rotation | 0.29 in. | 0.31 in. |
| $Y$ | 0.188 lb. | 0.190 lb. |
| $v$ | $3.62\times10^{-5}$ in. | $2.8\times10^{-5}$ in. |
| Pressure distribution on $mn$ | $C_1$ | $C_2$ |

FIG. 4. *Conical model under transverse load.*

The definitions of $C$ and $D$ are given in II, whence from (5.7),

$$(5.10) \qquad v=-35.4\times10^{2}\frac{Yh^{3}\nu^{2}}{4E\cos\alpha}, \qquad \omega_3=19.0\times10^{2}\frac{Yh^{3}\nu^{3}}{4E},$$

where the units of measurement are the pound and inch.

Now $E=219$ lb. in.$^{-2}$, and when the biting edge is acted upon by the critical transverse load (0.188 lb.) it undergoes a displacement $\delta$ and

$$(5.11) \qquad \delta=v+b\omega_3,$$
$$=3.62\times10^{-5}\text{ in.}$$

The corresponding displacement in the case of the incompressible membrane is $\delta=2.80\times10^{-5}$ in.

The centre of rotation of the tooth is at a distance $x'$ from the apex where $v+x'\omega_3=0$, whence $x'=-v/\omega_3$ and from (3.36) and (5.10) it is found that $x'=0.29$ in. Since the axial length of the root is 0.48 in. the following result is obtained.

V. When the conical model is subjected to a transverse load applied at the biting edge, the centre of rotation divides the root approximately in the ratio of two to three and is farthest from the apex.

This result agrees roughly with that of R. Kronfeld (5, p. 1270).

## 6. Discussion

There are blood capillaries in the periodontal membrane. The blood is squeezed out of those parts of the membrane where the blood pressure is exceeded by the pressure due to the external load on the tooth. There is said to be strangulation of the membrane in such regions. From Fig. 3 it is seen that, if axial load is steadily increased from zero, strangulation will first appear at the apex of the root. From Fig. 4 it is seen that, if transverse load is steadily increased from zero, strangulation will first appear at $M$ and $N$. Computation shows that strangulation will be produced in small regions surrounding these points by a transverse load of 3 gm. Schwarz (7) conducted experiments on the teeth of dogs and found that the symptoms of strangulation appeared for a transverse load of 5 gm. This agreement is quite good, as the teeth of dogs differ in shape from those of humans.

The periodontal membrane contains a large number of small fibres running from the tooth to the jaw-bone. It is commonly believed among dentists that the resistance against displacement of a loaded tooth is supplied by tension in these fibres (4, pp. 336–337). In this paper it is found that the resistance is attributed to the pressure in the membrane, and the agreement in the previous paragraph between calculated and empirical results substantiates this claim.

## Acknowledgments

The author wishes to thank Prof. J. L. Synge for much assistance, rendered personally and derived from his paper (8). Thanks are also due to Prof. W. J. Webber for the contents of Appendix B.

## Appendix A

*To obtain a solution in series of the equation*

$$\zeta_1^2\frac{d^2\psi}{d\zeta_1^2}+\zeta_1\frac{d\psi}{d\zeta_1}-(4n^2+\zeta_1^2)\psi=\zeta_1^3, \tag{A.1}$$

*where n is an integer.*

This equation has a solution of the form

$$\psi=\sum_{s=3}^{\infty} b_s\zeta_1^s, \tag{A.2}$$

if $b_s$ satisfy the equations

$$\text{(A.3)} \quad \begin{cases} b_3(3^2-4n^2)=1, \\ b_4(4^2-4n^2)=0, \\ b_s(s^2-4n^2)-b_{s-2}=0, \qquad (s=5, 6, \ldots). \end{cases}$$

If

$$\text{(A.4)} \qquad b_s=0, \qquad (s=4, 6, \ldots),$$

then a solution of (A.1) is

$$\text{(A.5)} \qquad \psi=\sum_{m=1}^{\infty} \frac{\zeta_1^{2m+1}}{\prod_{r=1}^{m}\{(2r+1)^2-4n^2\}}.$$

## Appendix B

*To obtain a solution in series of the equation*

$$\text{(B.1)} \qquad \zeta_1^2\frac{d^2\chi}{d\zeta_1^2}+\zeta_1\frac{d\chi}{d\zeta_1}-(4n^2+\zeta_1^2)\chi=\zeta_1^2,$$

*where n is an integer.*

If an attempt is made as in Appendix A to obtain a solution of the form

$$\text{(B.2)} \qquad \chi=\sum_{s=2}^{\infty} a_s\zeta_1^s,$$

it is found that

$$\text{(B.3)} \qquad a_{2(n+t)}=\infty, \qquad (t=0, 1, 2, \ldots),$$

and so some modification is necessary.

The equation

$$\text{(B.4)} \qquad \zeta_1^2\frac{d^2\chi_{+\epsilon}}{d\zeta_1^2}+\zeta_1\frac{d\chi_{+\epsilon}}{d\zeta_1}-(4n^2+\zeta_1^2)\chi_{+\epsilon}=\zeta_1^{2+\epsilon}, \quad \epsilon<<1,$$

has a solution of the form

$$\text{(B.5)} \qquad \chi_{+\epsilon}=\sum_{s=2}^{\infty} c_s\zeta_1^{s+\epsilon}$$

if

$$\text{(B.6)} \quad \begin{cases} c_2\{(2+\epsilon)^2-4n^2\}=1, \\ c_3\{(3+\epsilon)^2-4n^2\}=0, \\ c_s\{(s+\epsilon)^2-4n^2\}-c_{s-2}=0, \qquad (s=4, 5, \ldots). \end{cases}$$

Thus

$$\text{(B.7)} \qquad c_s=0, \qquad (s=3, 5, 7, \ldots),$$

and so

$$\chi_{+\epsilon}=\sum_{m=1}^{\infty}\frac{\zeta_1^{2m+\epsilon}}{\prod_{r=1}^{m}\{(2r+\epsilon)^2-4n^2\}}. \tag{B.8}$$

Since $(2n+\epsilon)^2-4n^2=\epsilon(4n+\epsilon)$, then

$$\chi_{+\epsilon}=\sum_{m=1}^{n-1}\frac{\zeta_1^{2m+\epsilon}}{\prod_{r=1}^{m}\{(2r+\epsilon)^2-4n^2\}}+\frac{\zeta_1^{\epsilon}}{\epsilon}\phi(\epsilon), \tag{B.9}$$

where

$$\phi(\epsilon)=\frac{1}{(4n+\epsilon)\prod_{r=1}^{n-1}\{(2r+\epsilon)^2-4n^2\}}\left[\zeta_1^{2n}+\sum_{m=n+1}^{\infty}\frac{\zeta_1^{2m}}{\prod_{r=n+1}^{m}\{(2r+\epsilon)^2-4n^2\}}\right]. \tag{B.10}$$

Now

$$\zeta_1^{\epsilon}=1+\epsilon\log_e\zeta_1+\frac{\epsilon^2(\log_e\zeta_1)^2}{2!}+\ldots, \tag{B.11}$$

whence

$$\chi_{+\epsilon}=\sum_{m=1}^{n-1}\frac{\zeta_1^{2m+\epsilon}}{\prod_{r=1}^{m}\{(2r+\epsilon)^2-4n^2\}}+\left\{\frac{1}{\epsilon}+\log_e\zeta_1+\ldots\right\}\left\{\phi(0)+\epsilon\left(\frac{\partial\phi}{\partial\epsilon}\right)_{\epsilon=0}+\ldots\right\}. \tag{B.12}$$

Similarly by changing the sign of $\epsilon$ a function $\chi_{-\epsilon}$ can be obtained. Hence a solution of

$$\zeta_1^2\frac{d^2\chi_\epsilon}{d\zeta_1^2}+\zeta_1\frac{d\chi_\epsilon}{d\zeta_1}-(4n^2+\zeta_1^2)\chi_\epsilon=\tfrac{1}{2}(\zeta_1^{2+\epsilon}+\zeta_1^{2-\epsilon}) \tag{B.13}$$

is

$$\begin{aligned}\chi_\epsilon&=\tfrac{1}{2}(\chi_{+\epsilon}+\chi_{-\epsilon}),\\&=\tfrac{1}{2}\sum_{m=1}^{n-1}\left[\frac{\zeta_1^{2m+\epsilon}}{\prod_{r=1}^{m}\{(2r+\epsilon)^2-4n^2\}}+\frac{\zeta_1^{2m-\epsilon}}{\prod_{r=1}^{m}\{(2r-\epsilon)-4n^2\}}\right]\\&\quad+\phi(0)\log_e\zeta_1+\left(\frac{\partial\phi}{\partial\epsilon}\right)_{\epsilon=0}+\epsilon^2[\ldots\ldots]+\ldots.\end{aligned} \tag{B.14}$$

By letting $\epsilon\to 0$ simultaneously in (B.13) and (B.14) it is found that a solution of (B.1) is

$$\begin{aligned}\chi&=\lim_{\epsilon\to 0}\chi_\epsilon,\\&=\sum_{m=1}^{n-1}\frac{\zeta_1^{2m}}{\prod_{r=1}^{m}\{(2r)^2-4n^2\}}+\phi(0)\log_e\zeta_1+\left(\frac{\partial\phi}{\partial\epsilon}\right)_{\epsilon=0},\end{aligned}$$

or

$$\text{(B.15)}\qquad \chi = \sum_{m=1}^{n-1} \frac{\zeta_1^{2m}}{\prod_{r=1}^{m} \{(2r)^2 - 4n^2\}}$$

$$+ \frac{\log_e \zeta_1}{4n \prod_{r=1}^{n-1} \{(2r)^2 - 4n^2\}} \left[ \zeta_1^{2n} + \sum_{m=n+1}^{\infty} \frac{\zeta_1^{2m}}{\prod_{r=n+1}^{m} \{(2r)^2 - 4n^2\}} \right]$$

$$- \sum_{m=n}^{\infty} \left[ \frac{1}{4n} + \sum_{r=1}^{m}{}' \frac{4r}{(2r)^2 - 4n^2} \right] \frac{\zeta_1^{2m}}{4n \prod_{r=1}^{m}{}' \{(2r)^2 - 4n^2\}},$$

where the dash on the $\Sigma$ and $\Pi$ signs means that the terms $r = n$ are to be omitted.

## References


1. BLACK, G. V. Dental anatomy. S. S. White Dental Manufacturing Co., Philadelphia. 1902.
2. DYMENT, M. L. and SYNGE, J. L. Oral Health, 25:105-109. 1935.
3. HAY, G. E. Can. J. Research, A, 17 : 106-121. 1939.
4. KRONFELD, R. Histopathology of the teeth and their surrounding structures. Lea and Febigen, Philadelphia. 1933.
5. KRONFELD, R. J. Am. Dental Assoc. 18 : 1242-1274. 1931.
6. ORBAN, B. Dental histology and embryology. P. Blakiston's and Co., Philadelphia. 1929.
7. SCHWARZ, A. M. Intern. J. Orthodontia, Oral Surgery and Radiography, 18 : 331-352. 1932.
8. SYNGE, J. L. Phil. Trans. Roy. Soc. Lond. A, 231 : 435-477. 1933.

# THE RESONANT RADIAL FREQUENCIES OF A CYLINDER OF ANY WALL THICKNESS[1]

By G. S. Field[2]


## Abstract

Equations have been derived for the resonance radial frequencies of a cylinder of any wall thickness. For the degenerate case of the internal radius equal to zero, the equations are shown to reduce to those previously given for a solid rod. For a cylinder with a very thin wall, the frequency equation becomes very simple, but contains an additional factor compared with the equation usually given for a thin-walled cylinder. It is suggested that the two cases correspond to slightly different types of vibration, and that the one considered in this paper is physically more likely.


## Radial Particle Velocity

In a previous paper (1) it was shown that for an element of a solid cylindrical rod, the expression for the radial particle velocity is,

$$\zeta = BJ_1(kr)e^{i\omega(t-z/c_1)},$$

where, $\zeta$ = radial particle velocity at a distance $r$ from the centre of the rod;
$B$ = constant of integration;
$\omega$ = $2\pi \times$ frequency;
$t$ = time;
$z$ = distance along the length of the rod;
$c_1$ = phase velocity of longitudinal wave in the rod;
$J_1(kr)$ = Bessel function of the first kind, and is a solution of the following equation:

$$r^2 \frac{\partial^2 f_2}{\partial r^2} + r \frac{\partial f_2}{\partial r} + (k^2r^2 - 1)f_2 = 0,$$

in which $k$ is a function of $c_1$, $\omega$, Young's modulus ($q$), the density ($\rho$), and Poisson's ratio ($\sigma$), but is independent of $r$.

The complete solution of Bessel's equation, above, includes Bessel's function of the second kind, *i.e.*, $Y_1(kr)$*, but for the solid rod this solution is not admissible, as $Y_1(kr)$ becomes infinite at $r = 0$.

For a hollow cylinder, however, $Y_1(kr)$ must be included, and the expression for the radial particle velocity becomes,

$$\zeta = [AJ_1(kr) + BY_1(kr)]e^{i\omega(t-z/c_1)}. \qquad (1)$$

## Axial Force on an Element

The equation for the axial force, $p_2$, along a radius vector, on an element in the wall of the cylinder, may be put in the following form (1, p. 257),

$$p_2 = \frac{q}{(1+\sigma)(1-2\sigma)}\left[\frac{\partial \zeta}{\partial r}(1-\sigma) + \sigma\left(\frac{\partial \xi}{\partial z} + \frac{\partial \eta}{\partial \theta} + \frac{\zeta}{r}\right)\right], \qquad (2)$$

[1] *Manuscript received March 28, 1939.*
*Contribution from the Division of Physics, National Research Laboratories, Ottawa, Canada. Issued as N.R.C. No. 821.*

[2] *Physicist, National Research Laboratories, Ottawa.*

* *$Y_n(x)$ was adopted as the canonical function of the second kind by Weber (3, p. 64) and is the most useful in the present case.*

where,

$\xi$ = longitudinal particle velocity at a distance $z$ along the axis;

$\eta$ = tangential particle velocity corresponding to the cylindrical co-ordinate $\theta$.

If only radial vibrations are considered, $\frac{\partial \xi}{\partial z} = \frac{\partial \eta}{\partial \theta} = 0$, and,

$$p_2 = \frac{q}{(1+\sigma)(1-2\sigma)}\left[\frac{\partial \zeta}{\partial r}(1-\sigma) + \sigma\frac{\zeta}{r}\right]. \tag{3}$$

## Boundary Conditions

Let the external radius of the hollow cylinder be $a_1$ and the internal radius be $a_2$. Then,

At $r = a_1$, $p_2 = 0$;

At $r = a_2$, $p_2 = 0$.

Substitute in Equation (3) for $\zeta$ and $r$. Then,

$$\left[\begin{array}{l} A[kr(1-\sigma)J_0(kr) - (1-2\sigma)J_1(kr)] \\ \qquad +B[kr(1-\sigma)Y_0(kr) - (1-2\sigma)Y_1(kr)] \end{array}\right]_{\substack{r=a_1 \\ r=a_2}} = 0. \tag{4}$$

Let $ka_1 = x$,

Then $ka_2 = (a_2/a_1)x$.

Divide each equation by $B(1-\sigma)$.

Write, $m = \frac{1-2\sigma}{1-\sigma}$ and $F = A/B$.

Finally,

$$F[xJ_0(x) - mJ_1(x)] + xY_0(x) - mY_1(x) = 0, \tag{5}$$

and

$$F[(a_2/a_1)xJ_0(a_2x/a_1) - mJ_1(a_2x/a_1)] + (a_2/a_1)xY_0(a_2x/a_1) - mY_1(a_2x/a_1) = 0. \tag{6}$$

From these equations it is possible to determine $F$ and $x$.

## Frequency Equation

The expression determining the resonant radial frequencies is (1, p. 259),

$$f = k\alpha/2\pi, \tag{7}$$

where, $f$ = frequency of resonant radial vibration;

$$\alpha = \sqrt{\frac{\text{extensional modulus of elasticity}}{\text{density}}}$$

$$= \sqrt{\frac{q(1-\sigma)}{(1+\sigma)(1-2\sigma)\rho}}.$$

Since $ka_1 = x$,

$$f = \frac{xa}{2\pi a_1} \tag{8}$$

## Solution of Equations in $x$ and $F$

In Equations (5) and (6), $F$ may readily be eliminated; this leaves an equation containing only $x$ and functions thereof. It is possible to solve this equation for any ratio of $a_2/a_1$ by substituting for different values of $x$ the values of the Bessel functions as given in the published tables.

A simpler method of solution is a graphical one. In Equation (5) denote $F$ by $F_5$, and in Equation (6) write $F$ as $F_6$.

$$F_5 = -\frac{xY_0(x) - mY_1(x)}{xJ_0(x) - mJ_1(x)} = -\frac{N}{D}, \tag{9}$$

$$F_6 = -\frac{(a_2/a_1)xY_0(a_2x/a_1) - mY_1(a_2x/a_1)}{(a_2/a_1)xJ_0(a_2x/a_1) - mJ_1(a_2x/a_1)} = -\frac{H}{G}. \tag{10}$$

From these equations, values of $x$ may be determined from the intersections of $F_5$ and $F_6$. By a consideration of the change-over points, where either the numerator or denominator of each equation equals zero, that is, where $F_5$ or $F_6$ changes sign, the ranges of $x$ where solutions are possible may be very greatly reduced. As an illustration of the method, definite values of $m$ and of the ratio $a_2/a_1$ may be taken.

Consider the values of $x$ for which solutions are possible.

Assume $\sigma = 0.226$, from which $m = 0.709$, and assume $a_2/a_1 = 0.8$. Table I may then be set up.

TABLE I

| $x$ | $N$ | $D$ | $H$ | $G$ | $F_5$ | $F_6$ | Possible solution ($F_5 = F_6$) marked + |
|---|---|---|---|---|---|---|---|
| 0 – 2.04 | + | + | + | + | − | − | + |
| 2.04 | + | 0 | + | + | $-\infty$ | − | |
| 2.04 – 2.55 | + | − | + | + | + | − | |
| 2.55 | + | − | + | 0 | + | $-\infty$ | |
| 2.55 – 3.76 | + | − | + | − | + | + | + |
| 3.76 | 0 | − | + | − | 0 | + | |
| 3.76 – 4.70 | − | − | + | − | − | + | |
| 4.70 | − | − | 0 | − | − | 0 | |
| 4.70 – 5.39 | − | − | − | − | − | − | + |
| 5.39 | − | 0 | − | − | $-\infty$ | − | |
| etc. | etc. | | etc. | | etc. | | |

From this table it will be observed that there are only a few ranges of $x$ where solutions are possible. It would be expected that in the first range would be found the solution giving the fundamental resonance frequency;

in the second, the solution for the first overtone; in the third, the second overtone; and so on.

By plotting a few points for $F_5$ and $F_6$ in each range, the form of each curve may be readily obtained. From the intersection of the curves, the desired solution of $x$ is determined and hence the resonant frequency. In Fig. 1 the curves for a particular case are given.

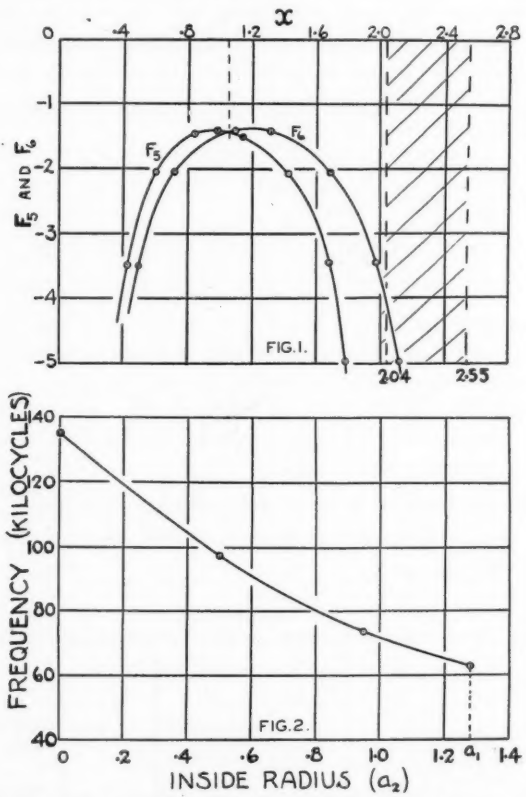


FIG. 1. *Curves of $F_5$ and $F_6$, illustrating graphical solution for $x$. $m = 0.709$, $a_2/a_1 = 0.8$.*

FIG. 2. *Curve showing changes in the resonant radial frequency of a cylinder with changes in the internal radius. Cylinder made of glass, external radius, 1.28 cm. Constants of glass as follows: $q = 6.4 \times 10^{11}$, $\rho = 2.6$, $\sigma = 0.226$.*

A number of resonant radial frequencies were calculated for values of $x$ determined as above, to show the variation in frequency with variations in the ratio $a_2/a_1$. In Fig. 2 these are plotted against $a_2$.

### Limiting Case of the Solid Rod ($a_2 \to 0$)

In $F_6$ write $(a_2/a_1)x = y$.

When $a_2 \to 0$, $y \to 0$, $J_0(y) \to 1$, $J_1(y) \to 0$ and $G \to 0$.

Hence $F_6 \to \infty$, unless $H \to 0$, in which case $F_6$ becomes indeterminate.

Suppose $H \to 0$ as $y \to 0$. Then,

$$\underset{y \to 0}{Lim}\left(yY_0(y)\right) = \underset{y \to 0}{Lim}\left(mY_1(y)\right).$$

When $y \to 0$, $Y_0(y) \to -\infty$. Hence, for $y \to 0$, $yY_0(y)$ can be put in the form $\infty/\infty$. Remembering that for this indeterminate form the limit of the quotient is equal to the limit of the quotient of the derivative of the numerator and the derivative of the denominator, the following may be obtained.

$$\underset{y \to 0}{Lim}\left(yY_0(y)\right) = \underset{y \to 0}{Lim}\left(\frac{Y_0(y)}{1/y}\right) = \underset{y \to 0}{Lim}\left(\frac{-Y_1(y)}{-1/y^2}\right) = \underset{y \to 0}{Lim}\left(y^2Y_1(y)\right).$$

Then,

$$\underset{y \to 0}{Lim}\left(y^2Y_1(y)\right) = \underset{y \to 0}{Lim}\left(mY_1(y)\right).$$

But, since the limit of the product of a finite number of quantities is equal to the product of their limits,

$$\underset{y \to 0}{Lim}\left(y^2Y_1(y)\right) = \left[\underset{y \to 0}{Lim}\,(y^2)\right] \times \left[\underset{y \to 0}{Lim}\left(Y_1(y)\right)\right]$$

$$= \left[\underset{y \to 0}{Lim}\,(m)\right] \times \left[\underset{y \to 0}{Lim}\left(Y_1(y)\right)\right].$$

Hence,

$$\underset{y \to 0}{Lim}\,(m) = \underset{y \to 0}{Lim}\,(y^2),$$

which is obviously untrue.

Therefore, as $a_2 \to 0$, $H$ does not $\to 0$, and $F_6 \to \infty$.

Since $F_5 = F_6$, as $a_2 \to 0$, $F_5 \to \infty$.

Hence, for $a_2 \to 0$,

$$xJ_0(x) - mJ_1(x) \to 0,$$

or,

$$xY_0(x) - mY_1(x) \to \infty.$$

Since $xY_0(x) - mY_1(x)$ can approach infinity only for $x \to 0$, the only useful solution for $x$ is contained in the expression,

$$xJ_0(x) \to mJ_1(x).$$

It has previously been shown (1, p.259) that the frequencies of radial resonance of a solid rod are given by the equation,

$$xJ_0(x) = mJ_1(x),$$

so that for the limiting case ($a_2 \to 0$) the equations developed in this paper are seen to degenerate to the correct form.

**Limiting Case of the Cylinder with Infinitely Thin Walls ($a_2 \rightarrow a_1$)**

Write $(a_2/a_1)x = x - h$.

Then, $h = (1 - a_2/a_1)x$,

and, as $a_2 \rightarrow a_1$, $h \rightarrow 0$.

From Taylor's theorem,

$$f(x - h) = f(x) - hf'(x) + \frac{h^2}{2!}f''(x) - \ldots .$$

By means of this equation, $F_6$ becomes,

$$\frac{(x - h)[Y_0(x) - hY_0'(x)] - m[Y_1(x) - hY_1'(x)]}{(x - h)[J_0(x) - hJ_0'(x)] - m[J_1(x) - hJ_1'(x)]},$$

in which expression $h^2$ and higher powers of $h$ have been neglected, since only those values of $h$ that approach zero are considered.

To obtain the desired solution for $x$, $F_6$ is to be equated to $F_5$, as follows. To simplify writing the equations, $J_0$ is written for $J_0(x)$, $Y_0$ is written for $Y_0(x)$, and so on.

$$\frac{(x - h)[Y_0 - hY_0'] - m[Y_1 - hY_1']}{(x - h)[J_0 - hJ_0'] - m[J_1 - hJ_1']} = \frac{xY_0 - mY_1}{xJ_0 - mJ_1}. \tag{11}$$

In the preceding equation, if the various derivatives are written in and the terms in $J_0$, $J_1$, $Y_0$, and $Y_1$, are collected, the following is obtained.

$$\frac{(x - h + mh)Y_0 + \left(hx - h^2 - m - \frac{mh}{x}\right)Y_1}{(x - h + mh)J_0 + \left(hx - h^2 - m - \frac{mh}{x}\right)J_1} = \frac{xY_0 - mY_1}{xJ_0 - mJ_1}. \tag{12}$$

This equation reduces to,

$$Y_0J_1\left\{x\left(hx - h^2 - m - \frac{mh}{x}\right) + m(x - h + mh)\right\}$$

$$= J_0Y_1\left\{x\left(hx - h^2 - m - \frac{mh}{x}\right) + m(x - h + mh)\right\}. \tag{13}$$

Hence,

$$Y_0J_1 = J_0Y_1, \tag{14}$$

or,

$$x\left(hx - h^2 - m - \frac{mh}{x}\right) + m(x - h + mh) = 0. \tag{15}$$

The only solution of Equation (14) is $x = \infty$, because,

$$J_{n-1}(x)Y_n(x) - J_n(x)Y_{n-1}(x) = \frac{2}{\pi x}.$$

Hence only Equation (15) need be considered.

Equation (15) reduces to,

$$x^2 = m(2 - m), \tag{16}$$

if $h^2$ is neglected.

The radial frequency is,

$$f = \frac{x\alpha}{2\pi a_1} = \frac{1}{2\pi a_1}\sqrt{\frac{q(1-\sigma)}{\rho(1+\sigma)(1-2\sigma)}} \times \frac{1-2\sigma}{1-\sigma}\left(2 - \frac{1-2\sigma}{1-\sigma}\right), \tag{17}$$

since,

$$m = \frac{1-2\sigma}{1-\sigma}.$$

Equation (17) reduces to,

$$f = \frac{1}{2\pi a_1}\sqrt{\frac{q}{\rho}} \cdot \sqrt{\frac{1}{1-\sigma^2}}. \tag{18}$$

This is not quite the equation ordinarily given (2, p. 138; for the case $s = 0$) for the frequency of free radial vibration of a thin-walled cylinder, as it contains the additional factor, $\sqrt{\frac{1}{1-\sigma^2}}$. As the value of Poisson's ratio usually varies between $\frac{1}{4}$ and $\frac{1}{3}$, the extra factor leads to an increased frequency of the order of about 3 to 6%. Practically this is of no very great significance, but the theoretical reason for the difference is interesting.

In the derivation of the above equations, a wave going from the inside of the cylinder wall to the outside of the wall, thence being reflected back towards the inside, and then being further reflected, was considered. In the derivation of the equation for the thin-walled cylinder, a simple extensional vibration of the tube wall is assumed; the phase of any element in the wall along the same radius vector is the same.

From what has just been said it will be realized that the type of vibration is essentially different in the two cases. Physically, the radial vibration of a cylinder must always be excited by an alternating pressure on the inside or on the outside of the wall, so that it is the type of vibration discussed in this paper that must occur. The frequency given by the simple theory is thus only an approximation to the correct value.

## References

1. FIELD, G. S. Can. J. Research, 11 : 254-263. 1934.
2. LAMB, H. The dynamical theory of sound. 2nd ed. E. Arnold. London. 1925.
3. WATSON, G. N. A treatise on the theory of Bessel functions. Cambridge University Press. 1922.

# Canadian Journal of Research

*Issued by* THE NATIONAL RESEARCH COUNCIL OF CANADA

VOL. 17, SEC. B. JULY, 1939 NUMBER 7


## A METHOD FOR THE DETERMINATION OF ORGANIC PHOSPHORUS IN SOILS AND SOIL EXTRACTS[1]


BY C. L. WRENSHALL[2] AND W. J. DYER[3]



### Abstract

Dissolved organic phosphorus may be determined, even in highly coloured alkaline soil extracts, by the application of photoelectric colorimetry to the ceruleomolybdate colour reaction of phosphate ions. Total organic phosphorus may be extracted from soil with 4 *N* hydrochloric acid followed by treatment of the residue with 3 *N* ammonium hydroxide. Inorganic phosphorus is determined by direct colorimetry in the acid extract and in the acidified alkaline extract. Total phosphorus is determined similarly in each extract after ignition. The difference between total and inorganic phosphorus is equivalent to the organically combined phosphorus content of the soil sample.

The soil organic phosphorus was found to be stable under these treatments. A considerable proportion of the organic phosphorus is extracted by acid, and the total soil phosphorus is almost completely extracted by the two treatments with 4 *N* hydrochloric acid and 3 *N* ammonium hydroxide.


### Introduction

One of the recent trends in soil chemistry is to resume the study of the soil phosphorus that is combined in organic compounds. This subject is being approached with two objectives; first, to obtain a better knowledge of the chemical combinations in which the soil phosphorus exists, and second, to explain the role of organic phosphorus in the complex cycle of phosphate in the soil. A review of the literature shows that no completely satisfactory method for the determination of organic phosphorus in soils and soil extracts has been proposed.

Parker and Fudge (6) applied the ceruleomolybdate colour reaction of phosphate ions to the determination of organic phosphorus in water extracts of soils. Inorganic phosphate was determined directly in an aliquot, and total phosphorus in another aliquot after ignition. The difference was taken to be organic phosphorus. This method was very limited in its application, since for visual colorimetry it was necessary to have colourless solutions.

Recently Dean (2) employed the same principle in determining organic phosphorus in alkaline soil extracts which he decolorized with kieselguhr or by treatment with bromine. Experiments in this laboratory indicate that complete decolorization is not attained by the action of bromine, and


[1] *Manuscript received February 16, 1939.*
*Contribution from the Faculty of Agriculture of McGill University, Macdonald College, Quebec, Canada, with financial assistance from the National Research Council of Canada. Macdonald College Journal Series No. 119.*



[2] *Lecturer in Chemistry, Macdonald College.*
[3] *Research Assistant, Department of Chemistry, Macdonald College.*

that the treatment with alkali and bromine is sufficiently drastic to release some phosphorus from organic combination.

Various methods have been proposed for determining total soil organic phosphorus by using the ceruleomolybdate reaction in conjunction with treatments designed to release phosphate from its organic linkage. Odynsky (5) determined the increase in acid soluble phosphate produced by igniting the sample. Recently Dickman and De Turk (3) published the details of a method based on releasing the organic phosphorus by treatment with hydrogen peroxide. In both these methods the whole soil is subjected to the destructive treatment and there is a danger that released phosphate may become fixed by the soil residue. Davis (1) has demonstrated that some soils may absorb phosphate from a medium with a pH value as low as 0.25. The usefulness of these methods is limited because they may not be applied to coloured solutions, such as alkaline soil extracts, where direct visual colorimetry is impracticable.

In a previous paper (4) the authors showed that it is possible to differentiate between organic and inorganic phosphorus in various soil extracts, including those containing coloured organic matter, by the use of a photoelectric colorimeter. It was thought that if all the organic phosphorus of soil could be brought into solution by suitable means, a determination of the total organic phosphorus could be effected. Such an approach proved feasible, and resulted in the method described herein. The method has been used with practical success since September, 1937.

## Procedure

### *A. Extraction*

A 1 gm. sample of finely ground soil (100 mesh) is placed in a 50 ml. Erlenmeyer flask and treated with 25 ml. of 4 *N* hydrochloric acid (redistilled). The contents are mixed by gentle rotation several times during the first hour, and then allowed to stand overnight. The mixture is filtered through hardened filter paper, and the residue washed with hot 0.01 *N* hydrochloric acid, it being completely transferred to the filter in the process. Washing with pure water sometimes causes peptization of organic matter. The filtrate is collected in a 100 ml. volumetric flask, cooled, and diluted to volume.

The residue from the acid extraction is then washed into a 100 ml. volumetric flask containing 20 ml. of concentrated ammonium hydroxide, and diluted to volume. The flask is stoppered and the contents are mixed several times during an hour, and allowed to stand until the following day. A quantity of this extract is centrifuged at moderate speed (3000 r.p.m.) for a few minutes to remove suspended material before aliquots are withdrawn for analysis.

### *B. Preparation for Total Phosphorus Determination*

A 10 ml. aliquot of the extract is placed in a silica evaporating dish containing 10 ml. of 1 *N* magnesium nitrate solution, and evaporated to dryness. Organic matter is completely destroyed by ignition at 550° C. After the dish has cooled sufficiently, 10 ml. of 1 *N* hydrochloric acid is added, and the

covered dish is placed on the steam bath for two hours to bring about complete hydrolysis to orthophosphate. The contents of the dish are then washed into a 100 ml. volumetric flask and one drop of paranitrophenol indicator (0.5% solution in water) is added. The pH of the solution is adjusted to approximately 3.0 by adding dropwise 1 *N* ammonium hydroxide until the appearance of a yellow colour, then discharging the yellow colour with a drop of 1 *N* hydrochloric acid. The solution is diluted to volume. A suitable aliquot, usually 25 ml., is transferred to a 50 ml. volumetric flask, and 2 ml. of the Truog and Meyer (10) acid molybdate reagent is added; this final solution is diluted to volume, and is then ready for the colorimetric determination.

*C. Preparation for Inorganic Phosphorus Determination*

*(1) On the acid extract.* A small aliquot, usually 5 ml., of the acid extract, is pipetted into a 50 ml. volumetric flask, diluted to 30 to 40 ml., the pH adjusted to approximately 3.0, and finally diluted to volume after the addition of 2 ml. of acid molybdate reagent, as described above.

*(2) On the alkaline extract.* A 10 ml. aliquot of the centrifuged extract is acidified by the dropwise addition of 4 *N* hydrochloric acid with continuous stirring. Acidification is complete when the flocculent precipitate of "humic acid" forms. The mixture is filtered into a 50 ml. volumetric flask, and the precipitate is washed with 0.01 *N* hydrochloric acid until the volume of filtrate is about 40 ml. The filtrate is adjusted to pH 3.0, and diluted to volume after the addition of 2 ml. of acid molybdate reagent.

*D. Colorimetric Procedure*

The photoelectric colorimetry of phosphorus in soil extracts has been discussed at length elsewhere (4, 9), and only an outline of the necessary manipulations is given here.

A 10 ml. aliquot of the final solution, containing acid molybdate reagent, is pipetted into a colorimeter tube. The tube is placed in the colorimeter, in which the 660 mμ filter has been inserted, and the rheostat so adjusted that the galvanometer shows a reading of 100*. One drop of 1% stannous chloride reagent is then added and mixed with the contents of the tube, and the galvanometer reading is recorded when the colour has developed to a maximum, which is usually about 10 min. after the addition of stannous chloride. The minimum galvanometer reading, corresponding to maximum colour, gives directly the concentration of phosphate phosphorus at the final dilution, by reference to calibration data. The appropriate calibration constant is obtained by measuring the light absorption in a phosphate solution of known concentration which contains the same concentration of ammonium chloride as the unknown.

The results in this paper are expressed as milligrams of phosphorus per gram of soil.

* *In reading a series of tubes it is convenient at this point to record the "centre setting", i.e., the galvanometer reading when the tube is removed. After the colours have been developed, adjustment to the appropriate centre setting is made for each tube before it is placed in the colorimeter for the final reading.*

## Results and Discussion

Some results obtained by the use of the method are presented in Table I. It may be seen from these data that a considerable proportion of the organic phosphorus is brought into solution by the acid extraction. On the other hand, following the action of relatively strong acid, the ammonia solution dissolves only slight traces of inorganic phosphorus. The sum of the amounts of phosphorus dissolved by the two extractions approaches the total phosphorus of the soil, the percentage extraction being from 90 to 100% in the typical instances reported. The almost complete recovery of the phosphorus in the muck soils indicates that the extraction of organic phosphorus is complete. The agreement between duplicate values for the proportion of the soil phosphorus that is organically combined appears to be very satisfactory, when it is considered that these values may combine the errors of four colorimetric phosphorus determinations. The analysis of an ignited sample offers convincing proof that the method gives a true representation of the organic-inorganic phosphorus distribution.

Further extraction with ammonia of the residue from mineral soils brings no more phosphorus into solution. It may be assumed that the phosphorus not dissolved by the two extractions is inorganic phosphorus contained in undecomposed mineral fragments. In one case the phosphorus content of the grey, silicious residue from the extraction of a mineral soil was determined, after magnesium nitrate fusion, and proved to be about 6% of the total soil phosphorus. This result is in harmony with the data for percentage extraction.

In order to ensure that no interfering substances or conditions were affecting the direct determinations of inorganic phosphorus, known amounts of phosphate were added to some of the extracts, and the recovery of these known additions was noted. It was found that the recovery was 99 to 100% in the acid extracts, but rather less satisfactory in the alkaline extracts, ranging from 95 to 100%. It was thought that the "humic acid" precipitate might be adsorbing inorganic phosphate. Some of these precipitates were dissolved in dilute ammonium hydroxide, reprecipitated, and the phosphate in the filtrate was estimated. The merest traces of phosphate were found, and it was concluded that inorganic phosphate is not adsorbed to an appreciable extent. Inorganic phosphate was determined directly in a dilute solution of the alkaline extract in some instances where the dissolved organic matter did not give too flocculent a precipitate upon acidification of the solution. The results were almost identical with those given by the filtration method. The difficulty in obtaining complete recovery of the phosphate in the alkaline extracts appears to be due mainly to the high concentrations of ammonium chloride present in these solutions. As shown elsewhere, ammonium chloride in high concentration not only depresses the colour intensity but also renders the colour less stable, so that it is almost impossible to perform quantitative colorimetry. However, the amount of phosphate involved in this particular determination is such a small proportion of the total phosphorus that the effect upon the result of the method as a whole is negligible.

## TABLE I

RESULTS OF ORGANIC PHOSPHORUS ANALYSES OF SEVERAL SOILS

| Soil type | Soil No. | * | Milligrams of phosphorus per gram of soil | | | | | | | | | Per cent extraction | Org. P, % of total P |
|---|---|---|---|---|---|---|---|---|---|---|---|---|---|
| | | | Acid extract | | | Ammonia extract | | | Total P ext. | Total org. P | Total P of soil** | | |
| | | | Total | Inorg. | Org. | Total | Inorg. | Org. | | | | | |
| Black muck | 1 | *a* | 0.490 | 0.100 | 0.390 | 0.466 | 0.013 | 0.453 | 0.956 | 0.843 | 0.970 | 98.6 | 86.9 |
| | | *b* | 0.490 | 0.099 | 0.391 | 0.455 | 0.017 | 0.438 | 0.945 | 0.829 | | 97.4 | 85.5 |
| | 2 | *a* | 0.585 | 0.220 | 0.365 | 0.384 | 0.013 | 0.371 | 0.969 | 0.736 | 0.980 | 98.9 | 75.1 |
| | | *b* | 0.612 | 0.220 | 0.392 | 0.380 | 0.008 | 0.372 | 0.992 | 0.764 | | 101.2 | 78.0 |
| Podsol | 3 | *a* | 0.562 | 0.317 | 0.245 | 0.150 | 0.009 | 0.141 | 0.712 | 0.386 | 0.780 | 91.3 | 49.5 |
| | | *b* | 0.562 | 0.317 | 0.245 | 0.150 | 0.009 | 0.141 | 0.712 | 0.386 | | 91.3 | 49.5 |
| | 4 | *a* | 0.410 | 0.230 | 0.180 | 0.170 | 0.000 | 0.170 | 0.580 | 0.350 | 0.610 | 95.1 | 57.4 |
| | | *b* | 0.400 | 0.220 | 0.180 | 0.168 | 0.002 | 0.166 | 0.568 | 0.346 | | 93.1 | 56.7 |
| Brown forest soil | 5 | *a* | 0.530 | 0.370 | 0.160 | 0.176 | 0.012 | 0.164 | 0.706 | 0.324 | 0.789 | 89.5 | 41.1 |
| | | *b* | 0.640 | 0.380 | 0.160 | 0.170 | 0.012 | 0.158 | 0.710 | 0.318 | | 90.0 | 40.3 |
| | 6 | *a* | 1.150 | 0.910 | 0.240 | 0.210 | 0.022 | 0.190 | 1.360 | 0.430 | 1.350 | 100.8 | 31.8 |
| | | *b* | 1.110 | 0.910 | 0.200 | 0.212 | 0.002 | 0.210 | 1.320 | 0.410 | | 97.8 | 30.4 |
| Ignited soil | 7 | *a* | 0.837 | 0.837 | 0.000 | 0.040 | 0.037 | 0.003 | 0.877 | 0.003 | 0.900 | 97.4 | 0.3 |
| | | *b* | 0.840 | 0.837 | 0.003 | 0.037 | 0.037 | 0.000 | 0.877 | 0.003 | | 97.4 | 0.3 |

* *a and b represent duplicate extractions.*

** *Separate determinations of the total phosphorus were made colorimetrically after magnesium nitrate fusions of the soils.*

It is known that organic phosphorus compounds are fairly stable in both acid and alkaline solutions at ordinary temperatures (7), and Schollenberger (8) showed that dilute ammonium hydroxide does not have any destructive action on the organic phosphorus compounds in soil. It was nevertheless thought important to test the stability of soil organic phosphorus in the presence of the relatively strong acid used for extraction. A series of analyses of an acid extract showed no change in the phosphorus distribution in a period of 10 days. The acid concentration of the final extract is, however, only 1 *N*, and an experiment was designed to compare the effects of different concentrations of acid applied directly to the soil in the usual procedure.

Hydrochloric acid was used at the following concentrations: 0.5 *N*, 1 *N*, 3 *N*, 5 *N*. The results are summarized in Table II.

There does not appear to be any consistent difference between the results obtained with different concentrations of acid. The use of 4 *N* acid seems to be quite reasonable in the light of these data; in fact, it is evident that the concentrations of the extracting acid may vary between wide limits without affecting the determination. It is felt that this fact is in strong support of the validity of the present method.

Table II shows that the total phosphorus extracted is appreciably more when 3 *N* or 5 *N* acid is used. The solubility of organic phosphorus in the acid solution increases progressively with the concentration of acid, and ammonia extraction removes the remainder in each case. The amount of

TABLE II

INFLUENCE OF THE CONCENTRATION OF THE EXTRACTING ACID ON THE DETERMINATION OF TOTAL ORGANIC PHOSPHORUS

| Concentration of extracting acid (HCl) | Milligrams of phosphorus per gram of soil* | | | | | | | | Per cent ext'n | Org. P, % of total P |
|---|---|---|---|---|---|---|---|---|---|---|
| | Acid extract | | | Ammonia extract | | | Total P ext'd | Total org. P | | |
| | Total | Inorg. | Org. | Total | Inorg. | Org. | | | | |
| 0.5 *N* | 0.255 | 0.207 | 0.048 | 0.455 | 0.052 | 0.403 | 0.710 | 0.451 | 91.0 | 57.8 |
| 1 *N* | 0.294 | 0.234 | 0.060 | 0.415 | 0.044 | 0.369 | 0.709 | 0.429 | 90.9 | 55.0 |
| 3 *N* | 0.467 | 0.287 | 0.180 | 0.290 | 0.020 | 0.270 | 0.757 | 0.450 | 97.0 | 57.7 |
| 5 *N* | 0.555 | 0.322 | 0.233 | 0.205 | 0.012 | 0.193 | 0.760 | 0.426 | 97.4 | 54.7 |

* *Soil No. 8—, a podsol, with a total P content (air dry) of 0.078%.*

inorganic phosphate in the ammonia extract decreases as the concentration of the extracting acid is increased. This observation favours the extraction with strong acid (3 to 5 *N*) since its use minimizes the errors of colorimetry in regard to the alkaline extract. Indeed, when the acid used is 3 *N* or stronger, only a minor error would be incurred by assuming that all the phosphorus of the ammonia extract is organic phosphorus. This suggests a means by which a very good estimate of the organic phosphorus may be obtained without the use of a photoelectric colorimeter, as visual colorimetry is feasible in the acid extract.

The results in Table I suggest an interesting relation between soil type and the proportion of phosphorus organically combined. In muck soils, which owe their existence to the inhibition of organic decay, the proportion of organic phosphorus is very high. In the podsols, where the organic matter is poorly decomposed, the proportion of organic phosphorus is intermediate, and in the brown forest soils, where the decomposition of organic matter is well advanced, the proportion of organic phosphorus is lowest. It is, perhaps, of interest that soil No. 6 is a very fertile soil, probably the most fertile of the group analyzed. However, the data at hand are too few to permit any definite conclusions to be drawn in this connection.

## References

1. Davis, L. E. Soil Sci. 40 : 129-158. 1935.
2. Dean, L. A. J. Agr. Sci. 28 : 234-246. 1938.
3. Dickman, S. R. and DeTurk, E. E. Soil Sci. 45 : 29-39. 1938.
4. Dyer, W. J. and Wrenshall, C. L. Can. J. Research, B, 16 : 97-108. 1938.
5. Odynsky, W. Sci. Agr. 16 : 652-664. 1936.
6. Parker, F. W. and Fudge, J. F. Soil Sci. 24 : 109-117. 1927.
7. Plimmer, R. H. A. Biochem. J. 7 : 72-80. 1913.
8. Schollenberger, C. J. Soil Sci. 6 : 365-395. 1918.
9. Smith, G. R., Dyer, W. J., Wrenshall, C. L., and De Long, W. A. Can. J. Research, B, 17 : 178-191. 1939.
10. Truog, E. and Meyer, A. H. J. Ind. Eng. Chem., Anal. Ed. 1 : 136-139. 1929.

# PRESSURE, VOLUME, TEMPERATURE RELATIONS OF ETHYLENE IN THE CRITICAL REGION. I.[1]

By J. Dacey[2], R. McIntosh[2], and O. Maass[3]

## Abstract

Pressure isothermals of the system were determined both above and below the temperature of disappearance of the meniscus. Regions of constant pressure with changing volume were observed with all isothermals, in agreement with the prediction of Mayer and Harrison (2, 3). The complete envelope of this region above the critical temperature has not as yet been determined. The pressure of the heterogeneous system at 9.50° C. was found to correspond within experimental error to the pressure of the flat portion of the homogeneous isothermal at the same temperature. The pressure of this heterogeneous system was found to be independent of the mass-volume ratio; this is in agreement with the experimental behaviour previously discovered by the authors (5) for such a system at 9.80° C. Moreover, the pressure of the heterogeneous system was found to be identical with that of the system which had been heated at constant volume to a temperature at which the density difference in the tube is known to have been destroyed, and then cooled to the same temperature of 9.50° C.

The isothermal at 9.60° C. was studied, and shown to be the equilibrium curve at that temperature. A hysteresis was observed on reversing the direction of measurement, *i.e.*, from "vapour" to compressed "liquid". This hysteresis was found to be caused by the time lags which are observed in passing from the "vapour" region of an isothermal to regions of high density. Certain apparent discrepancies between the work of the present authors and that of Geddes and Maass have been observed and cannot as yet be explained.

The phenomena observed are interpreted on the basis of a difference between the gaseous and liquid states of aggregation, with a structure assigned to the latter.

## Introduction

The present work is a continuation of that reported by McIntosh and Maass (5) on the density, pressure, and temperature relations of ethylene, and has been directed primarily toward the study of certain predictions made by Mayer and Harrison (2, 3) of the behaviour of condensing systems, and of the hypothesis of Maass that the liquid state of aggregation may persist above the temperature of disappearance of the meniscus and is characterized by a dynamic regional orientation.

Specifically, Mayer and Harrison have predicted the existence of a region above the critical temperature throughout which $\left(\frac{\partial P}{\partial V}\right)_T = 0$. This region has an upper limit at that isothermal for which $\left(\frac{\partial P}{\partial V}\right)_T = 0$ for one point only. The isothermals of Geddes and Maass (4) showed no such region. This can be explained on the assumption that the experimental points of the isobars, from which the isothermals were evaluated, were not taken with sufficiently small temperature increments.

[1] *Manuscript received February 28, 1939.*

*Contribution from Division of Physical Chemistry, McGill University, Montreal, Canada, with financial assistance from the National Research Council of Canada.*

[2] *Holder of a Studentship under the National Research Council of Canada.*

[3] *MacDonald Professor of Physical Chemistry, McGill University.*

In the present work, isothermals were determined experimentally at volume intervals as minute as possible, particularly throughout the volume ranges where flat portions of the curves might be expected. Relative pressures are determined to the limit of error that is inherent in the manual thermostatic control of the temperature of the carbon dioxide, that is, 0.01 atm. Within this limit the prediction of Mayer and Harrison has been verified. The data of these and other experiments are given below.

## Experimental

The apparatus used in this investigation has been adapted from the original design of Geddes and Maass (4). It consists of two Pyrex glass bombs, supported on brass rods, and connected from the bottoms by a U-tube of heavy walled Pyrex capillary. The apparatus is filled with pure mercury to about the half-way position in each bomb. This mercury acts as a piston in the manipulation of the ethylene, which is confined in the right-hand bomb, and also transmits the pressure generated by the carbon dioxide in the left-hand bomb. The carbon dioxide is added in the proper amount so that a two-phase system will be maintained through the volume and temperature ranges required. In these respects the apparatus of Geddes and Maass has been copied exactly. In the present arrangement, however, the spiral and float have been omitted, and differences in volume are recorded by the position of the mercury level as read upon a cathetometer scale. The internal diameters of the tubes were calibrated by measuring the height of known weights of pure mercury, and were found to be constant within the experimental error of the calibration. The determination of the absolute volume necessitated a geometric estimation of the volume of the draw-off; this was checked by repeating the determination of a point upon the isobars of McIntosh and Maass (5). The agreement was very good.

The absence of the spiral and float permitted the use of much narrower tubing, with consequent decrease in the danger of explosions. The inability with this design, to detect the presence of heterogeneous systems is not a great disadvantage, because the conditions under which these systems exist were well known from previous work, and the pressures of such systems were the point of interest rather than the actual density differences. Moreover, it was now possible to stir the ethylene by means of a magnetic stirring arrangement.

## Experimental Results

Five isothermals of the system ethylene were obtained and are represented in Fig. 1 and the values tabulated in Table I. The experimental procedure, the same in all cases, was as follows. The ethylene was compressed to a high density at 8.9° C. by adjustment of the carbon dioxide pressure. The temperature of the ethylene was then raised at constant volume to the temperature of the desired isothermal by balancing the change in pressure by further careful adjustment of the carbon dioxide pressure. After equilibrium had been attained, small decreases in the pressure were made and the equilibrium

TABLE I

PRESSURE-VOLUME-TEMPERATURE DATA

| Volume, cc. | Pressure, atm. | Volume, cc. | Pressure, atm. | Volume, cc. | Pressure, atm. |
|---|---|---|---|---|---|
| *Temperature, 8.92° C.* | | *Temperature, 9.22° C.* | | *Temperature, 9.42° C.* | |
| 2.532 | 49.93 | 2.590 | 50.18 | 2.710 | 50.26 |
| 2.587 | 49.73 | 2.613 | 50.06 | 2.735 | 50.15 |
| 2.672 | 49.54 | 2.655 | 49.96 | 2.838 | 50.06 |
| 2.893 | 49.45 | 2.715 | 49.87 | 2.950 | 50.02 |
| 3.271 | 49.45 | 2.794 | 49.85 | 3.176 | 49.99 |
| 3.681 | 49.46 | 2.830 | 49.80 | 3.300 | 49.99 |
| 4.303 | 49.38 | 2.970 | 49.75 | 3.550 | 49.97 |
| 4.317 | 49.34 | 3.284 | 49.75 | 3.723 | 49.94 |
| | | 3.666 | 49.73 | 3.910 | 49.90 |
| | | 3.876 | 49.72 | 4.104 | 49.85 |
| | | 4.006 | 49.68 | | |
| | | 4.174 | 49.65 | | |
| *Temperature, 9.50° C.* | | *Temperature, 9.60° C.* | | *Temperature, 9.60° C.* | |
| 2.705 | 50.42 | 2.695 | 50.52 | 4.000 | 50.10* |
| 2.722 | 50.32 | 2.713 | 50.45 | 3.958 | 50.16 |
| 2.762 | 50.22 | 2.756 | 50.34 | 3.903 | 50.20 |
| 2.789 | 50.19 | 2.854 | 50.27 | 3.782 | 50.23 |
| 2.829 | 50.17 | 3.135 | 50.18 | 3.586 | 50.29 |
| 2.908 | 50.12 | 3.360 | 50.17 | 3.148 | 50.34 |
| 2.970 | 50.10 | 3.512 | 50.15 | 2.858 | 50.36 |
| 3.235 | 50.08 | 3.607 | 50.14 | 2.753 | 50.42 |
| 3.455 | 50.07 | 3.710 | 50.13 | | |
| 3.624 | 50.06 | 3.859 | 50.09 | | |
| 3.857 | 50.03 | 4.020 | 50.05 | | |
| 4.197 | 49.90 | | | | |

* *Increasing pressure, thermal equilibrium only established.*

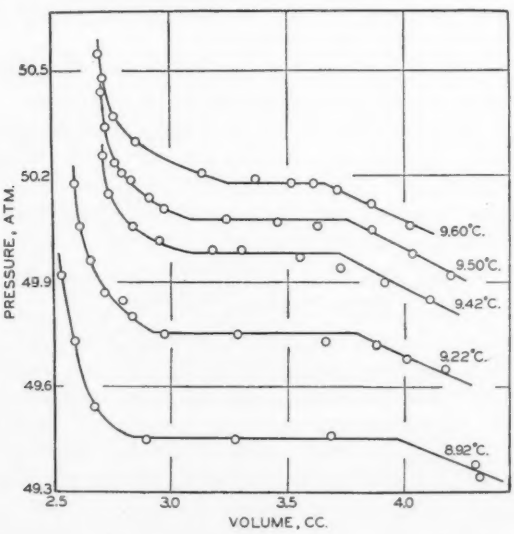


FIG. 1.

volumes determined from the mercury level as read upon the cathetometer scale. In that region where a horizontal part of the curve is shown, the decrease in pressure is exactly compensated for by the change in mercury level.

All isothermals showed a region wherein $\left(\frac{\partial P}{\partial V}\right)_T = 0$, although the isothermals at 9.50° C. and 9.60° C. are respectively at and 0.10° higher than the temperature at which the meniscus disappears. The envelope of this region has not yet been completely determined, but insofar as the work has been carried out, the prediction of Mayer and Harrison mentioned above has been verified.

*Isothermal at 9.60° C.*

Since the deduction of the existence of a two-phase system from the observation of a region wherein $\left(\frac{\partial P}{\partial V}\right)_T = 0$ is open to the objection that the behaviour of a one-phase system, if the compressibility is great enough, may simulate that of a two-phase system, and since the compressibility of liquids near the critical point is admittedly enormous, the direction of measurement of the points along the isothermal at 9.60° C. was reversed. That is, when the substance had been expanded to the last point on the isothermal, the pressure was increased. As soon as temperature equilibrium had been established, the pressure was maintained constant for 10 min. By following this procedure, the upper curve of Fig. 2 was obtained. This showed the compressibility

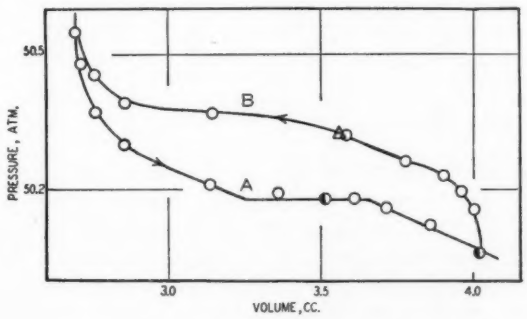


FIG. 2

of the system to be dependent upon its previous history. That the points of the lower curve are not dependent on the previous condition of the system, provided only that expansion into the true "gaseous" region has not occurred, was shown by repeating, several days later, the determination of a point on the flat portion of the curve. The procedure was as follows. The system was compressed to a high density, the temperature raised as previously described, and the pressure adjusted to the value corresponding to the flat portion of

the curve. Immediate expansion took place, and an equilibrium value was attained at the volume represented by the shaded circle. This point showed no change after more than 15 min. under these conditions. The pressure was then adjusted in order to repeat the last "vapour" point shown upon the diagram. This point (also shaded circle) was exactly repeated, and no tendency to change was exhibited at the end of 15 min.

The question whether the pressure on the higher curve would fall spontaneously to the value on the lower curve was then investigated. After expansion to the "gaseous" region of density the pressure on the system was adjusted to give the triangular point on the upper curve. When this point had been reached, the volume was maintained as constant as possible, and a pressure-time curve obtained. It was found that the pressure fell quite rapidly to the value of the original curve, where it remained constant. The difficulty of keeping the volume constant is very great, as the limit of adjustment of pressure is 0·01 atm., which represents a change of nearly 4 mm. in the height of the mercury. However, the volume can be kept constant enough to show clearly the true trend of the pressure with time. The figures are given in Table II.

TABLE II

| Volume | Temperature | Pressure | Time |
|---|---|---|---|
| 3.59 | 9.60 | 50.28 | 0 |
| 3.55 | 9.60 | 50.27 | 7 |
| 3.55 | 9.60 | 50.24 | 13 |
| 3.55 | 9.60 | 50.22 | 20 |
| 3.57 | 9.60 | 50.20 | 26 |
| 3.57 | 9.60 | 50.18 | 34 |
| 3.57 | 9.60 | 50.18 | 40 |

NOTE: *Zero time was taken at about 12 min. after the original pressure adjustment was made.*

The information obtained from these experiments indicates the interesting deduction that, as shown by Geddes and Maass, although compression destroys the macroscopic heterogeneity of the system, the two-phase character is re-formed by compression, even at a temperature 0.10° higher than the temperature of disappearance of the meniscus. This leads to the conclusion that over short ranges of temperature above that at which the meniscus becomes invisible, the nature of the system is determined by the density, or the mass-volume ratio. Further support of this statement may be derived from the following experiments.

*Pressure Measurements of the Heterogeneous and Homogeneous Systems at 9.50° C.*

The question of relative stability of the heating and cooling curves of such a typical isochore as appears in Fig. 3, as measured by the pressure of the systems over a range of density from below the critical density to well above it, was determined by the following series of experiments. The volume of

the system was fixed by freezing the mercury in the centre U-tube at a value of the average density where a heterogeneous system is known to exist from the previous work of McIntosh and Maass. The temperature of the ethylene was then raised to 9.50° C., the mercury melted, and the pressure of the system corresponding to a point upon the heating curve of the isochore determined.

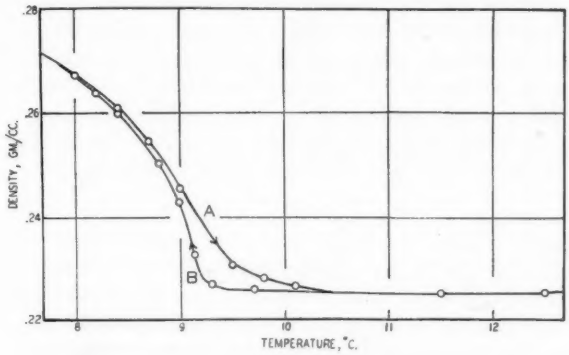


FIG. 3.

The mercury was then frozen, and the temperature raised to 11.5° C., where the density of the system has been shown to be constant. After sufficient time had been allowed for the medium to reach equilibrium, the temperature was again lowered to 9.50° C. and the pressure determined. It was shown that over the range of densities studied, the pressures shown by the upper curve, A, and lower curve, B, are identical, and are the same as the pressure corresponding to the 9.50° C. isothermal of the homogeneous system. The data are given in Table III. The pressures, although recorded to only 0.01

TABLE III

| Av. Dens. | $Pressure_A$ | $Pressure_B$ | Temp. |
|---|---|---|---|
| .1990 | 50.08 | 50.08 | 9.50 |
| .2040 | 50.08 | 50.08 | 9.50 |
| .2090 | 50.08 | 50.08 | 9.50 |
| .2173 | 50.08 | 50.08 | 9.50 |
| .2287 | 50.08 | 50.08 | 9.50 |

*Pressure of flat portion of homogeneous isothermal at 9.50 is 50.07 atm. Range of density of horizontal portion is 0.229 to 0.198 gm. per cc., approximately.*

atm., are more nearly equal than 0.01 atm. The reason for this statement is that, although changes in pressure can be determined with any degree of certainty only to that limit, smaller differences in pressure are shown by the change in mercury level on the cathetometer scale. That is, when a pressure measurement had been made during the determination of the heating

curve, A, the mercury frozen, and the conditions adjusted to give the point upon the cooling curve, B, and the mercury melted, no change in mercury level could be detected by means of the cathetometer.

The agreement between the pressure of the macroscopically heterogeneous system and that corresponding to the horizontal portion of the isothermal of the homogeneous system, together with the further similarity of density range throughout which the heterogeneous system is known to exist on the one hand, and throughout which the pressure of the homogeneous system is known to remain constant on the other hand, indicates that for these temperatures which exhibit horizontal regions on the pressure-volume curves, heterogeneous systems may be obtained, which are apparently stable and will show no tendency to change spontaneously to systems of a homogeneous character.

Further, apparently then, the flat portion of the cooling curve of a typical isochore cannot be regarded as representing a homogeneous gas system with the liquid structure destroyed, for such a gas system would have a pressure independent of the volume over quite appreciable ranges. It is concluded, therefore, that the system, although macroscopically homogeneous, is still a two-phase system, with the effect of the temperature being to disperse, or mix mechanically, the two phases. This opinion is in agreement with the conclusion reached by Naldrett, Mason and Maass from a study of critical opalesence which is to be published shortly. It also explains the observation of McIntosh and Maass (5) that the phase densities of ethylene at the critical temperature are dependent on the mass-volume ratio of the system. From this new point of view, the phase densities will be dependent on the amount of dilution of one phase by the other, which, as the meniscus rises or falls rapidly near the critical temperature, depending upon the value of the average density, will be a function of the mass-volume ratio.

*Effect of Mechanical Stirring upon the Pressure of the Heterogeneous System.*

In the design of apparatus used in this investigation it was possible to include a magnetic stirring arrangement in the ethylene side of the system. This was done in order to ascertain whether mechanical stirring, which has been emphasized as necessary in criticisms of work done in this laboratory, would affect the phenomena which are observed.

A heterogeneous system was therefore obtained at 9.50° C. and its pressure recorded. This system was then violently stirred by movement of the magnet up and down the length of the tube for a period of 20 sec. Several minutes were allowed to elapse, and the pressure was again recorded. This treatment was repeated four times. No change in pressure could be detected and the mercury level as read upon the cathetometer scale was unchanged. Although no mass movement of material could be detected during the stirring, the stirring was of sufficient violence to cause large visible transfers of liquid short distances into the vapour phase when the temperature was below the critical. This experiment lends strong support to the statement of McIntosh

and Maass that "mechanical stirring that does not cause local heating and cooling, or expansion and compression, does not influence the phenomena observed, either in kind or in rate of attainment of equilibrium."

Moreover, the fact that the phenomena reported in this paper, which are similar to those reported in previous publications from this laboratory, was observed in a tube that contained no spiral, completely refutes the argument of Ruedy (4) that the presence of a spiral acts as a deterrent to the proper mixing and diffusing of the system, and is the reason for the anomalous observations that have been made in the critical region.

*Apparent Discrepancies between Work of Geddes and Maass and Present Work*

A disagreement in the values of the critical pressure of ethylene has been found. Geddes and Maass found that the critical pressure depended upon the mass-volume ratio and reported the two values of 49.98 and 50.01 atm. at the average densities of 0.2056 and 0.2302 gm. per cc. respectively (5). The present work gives a critical pressure of 50.07 atm. over a density range of 0.198 to 0.220 gm. per cc. approximately. No attempt to explain this difference is considered feasible at the present stage of the work.

## References

1. GEDDES, A. L. Ph.D. Thesis, McGill University. 1936.
2. HARRISON, S. F. and MAYER, J. E. J. Chem. Phys. 6 : 87-100. 1938.
3. HARRISON, S. F. and MAYER, J. E. J. Chem. Phys. 6 : 101-104. 1938.
4. MAASS, O. and GEDDES, A. L. Phil. Trans. Roy. Soc. A, 236 : 303-332. 1937.
5. MCINTOSH, R. and MAASS, O. Can. J. Research, B, 16 : 289-302. 1938.
6. RUEDY, R. Can. J. Research, A, 16 : 89-99. 1938.